



**UNIVERSIDADE FEDERAL DO PARÁ
INSTITUTO DE GEOCIÊNCIAS
PROGRAMA DE PÓS-GRADUAÇÃO EM GEOLOGIA E GEOQUÍMICA**

DISSERTAÇÃO DE MESTRADO Nº 599

**FLORA E FAUNA DO NEÓGENO DAS ÁREAS DE
MANGUEZAIS DE LAGOAS COSTEIRAS DA
PLATAFORMA EQUATORIAL DO BRASIL: PROCESSO
DE PIRITIZAÇÃO**

Dissertação apresentada por:

GIOVANNI ALVARO TEIXEIRA DA MATA

Orientador: Prof. Dr. Orangel Antonio Aguilera Socorro (UFF)

**BELÉM - PARÁ
2021**

**Dados Internacionais de Catalogação na Publicação (CIP) de acordo com ISBD
Sistema de Bibliotecas da Universidade Federal do Pará
Gerada automaticamente pelo módulo Ficat, mediante os dados fornecidos pelo(a) autor(a)**

M425f Mata, Giovanni Alvaro Teixeira da.
Flora e fauna do neógeno das áreas de manguezais de lagoas costeiras da plataforma equatorial do Brasil: processo de piritização / Giovanni Alvaro Teixeira da Mata. — 2021.
xiv, 50 f. : il. color.

Orientador(a): Prof. Dr. Orangel Antonio Aguilera Socorro

Dissertação (Mestrado) - Universidade Federal do Pará, Instituto de Geociências, Programa de Pós-Graduação em Ciências Ambientais, Belém, 2021.

1. Geologia Sedimentar. 2. Formação Pirabas. 3. Fósseis Piritizados. I. Título.

CDD 551.30098



Universidade Federal do Pará
Instituto de Geociências
Programa de Pós-Graduação em Geologia e Geoquímica

**FLORA E FAUNA DO NEÓGENO DAS ÁREAS DE
MANGUEZAIS DE LAGOAS COSTEIRAS DA
PLATAFORMA EQUATORIAL DO BRASIL: PROCESSO
DE PIRITIZAÇÃO**

Dissertação apresentada por

GIOVANNI ALVARO TEIXEIRA DA MATA


Como requisito parcial à obtenção do Grau de Mestre em Ciências na Área de
GEOLOGIA, linha de pesquisa **ANÁLISE DE BACIAS SEDIMENTARES**

Data de aprovação: 02 / 04 / 2021

Banca Examinadora:



Prof. Dr. Orangel Antonio Aguilera Socorro
(Orientador – UFF)



Prof. Dr. Vinicius Tavares Kutter
(Membro – UFPA)



Prof. Dr. Renato Campello Cordeiro
(Membro-UFF)

Dedico este trabalho a minha família,
Como forma de agradecê-los pelo apoio incondicional.

AGRADECIMENTOS

À Deus, por me dar forças pra não desistir nos momentos difíceis e ajudar a enfrentar todas as barreiras e obstáculos.

A minha avó, Maria da Gloria, que mesmo não estando mais presente fisicamente nesta vida, continua emanando suas preces e orações.

Aos meus pais, Ody Tavares e Ivone Teixeira, pelo apoio incondicional nos instantes mais importantes e palavras de incentivo nos momentos mais difíceis, sempre reforçando que o melhor caminho para o sucesso é o estudo.

A minha namorada e amiga Bruna Gomes por todo apoio moral e afetivo, incentivando sempre a continuar e jamais baixar a cabeça, insistindo sempre na minha busca pelo melhor. Obrigado amor.

A Universidade Federal do Pará (UFPA) e ao programa de Pós-graduação em Geologia e Geoquímica (PPGG) pelo espaço de estudo cedido, pela infraestrutura fornecida e por toda equipe de direção que se esforça diariamente para que todo esse maquinário funcione ordenadamente.

A fundação de Coordenação e Aperfeiçoamento de Pessoal de Nível Superior (CAPES) pela bolsa de estudos e auxílio financeiro à pesquisa realizada no presente trabalho.

A equipe do Laboratório de Sedimentologia da UFPA, pela preparação das amostras. Ao Laboratório de Laminação da UFPA, pela confecção de lâminas. A equipe do Laboratório de Microanálise da UFPA, pelo auxílio na análise de MEV. A equipe do Laboratório de caracterização mineral da UFPA pela ajuda nas análises de difração de raios-x.

Ao Professor Dr. Orangel Antonio Aguilera que, mesmo trabalhando a distância não mediu esforços ao aceitar orientar-me, e com toda sua experiência profissional agregou ao presente trabalho enriquecedoras contribuições com sua visão científica e sobretudo pessoal.

Ao prof. Dr. Afonso Nogueira por assumir em grande parte deste percurso o papel de orientador, acompanhando o presente trabalho desde a pesquisa de campo até as precisas conclusões. Agradecer sua ajuda e determinação e sobretudo toda sua paciência e confiança a mim atribuída durante a elaboração desta dissertação. É um amigo e um grande profissional que a academia me deu a oportunidade de trabalhar.

Ao prof. Dr. Guilherme Rafaelli por assumi essa parceria, cobrando, exigindo e indicando o melhor caminho a percorrer. Sem dúvida um amigo que trouxe para o trabalho suas contribuições, críticas e discussões científicas mais importante para a evolução e finalização desta dissertação

Ao Alexandre Ribeiro (Maniçoba) pela contribuição técnica, mecânica e conceitual. Servindo como uma inspiração e funcionando, acima de tudo, como um amigo que tive o prazer de agregar ao trabalho.

A Prof. Dr. Ana Nogueira pela atenção dada desde a correção em cada apresentação de seminário até seu esforço para a coleta e preparação das amostras destinadas a análise de óptica.

Aos meus amigos, Lucy Soares, Luana Camile, Vitor Moura e Hiago Nery, que carregou desde a graduação como pessoas que sempre incentivaram a correr e buscar sempre o melhor.

Aos meus amigos de pós-graduação e do Grupo de Análises de Bacias Sedimentares da Amazônia (GSED), Mateus Xavier, Taynara Martins, Izabella, Renam, Hudson, Pedro e Walmir, por todo apoio e ajuda nas horas de dúvidas e conversas aleatórias em momentos de descontração

E aqueles que de forma direta ou indireta torcerem, incentivaram ou mesmo apoiaram durante a construção e desenvolvimento desta dissertação, meu muito obrigado.

“Talvez não tenha conseguido fazer o melhor, mas
lutei para que o melhor fosse feito.
Não sou o que deveria ser, mas Graças a
Deus, não sou o que era antes”.

Marthin Luther King

RESUMO

As rochas carbonato-siliciclásticas do início e meio da Formação Pirabas do Mioceno na margem equatorial do Brasil apresentam ecofácies salobras de paleoambientes de manguezais e lagoas costeiras sob influência das marés. A seção estudada possui lamito escuro no topo, caracterizado por uma zona de metanogênese microbiana onde troncos piritizados, folhas, micro e macrofósseis, e vestígios de fósseis, foram investigados. A caracterização petrográfica e as análises cristalográficas distinguem principalmente o cristal de framboids para fragmentos de tronco aos cristais octaédricos e cúbicos de conchas de invertebrados. As análises geoquímicas revelaram que o Fe e o S estão concentrados tanto no conteúdo fossilífero dos constituintes dos invertebrados quanto na matriz que hospeda o tronco, enquanto os demais elementos estão principalmente ligados aos invertebrados. A distribuição preferencial desses elementos está de acordo com a presença de compostos FeS_2 em substituição aos fósseis, refletindo as condições anóxicas e redutoras do meio ambiente. A seção litoestratigráfica rica em pirita foi depositada em um ambiente de águas rasas, onde a mineralização da pirita foi desenvolvida durante o estágio diagenético inicial sob condições anóxicas, abundância de matéria orgânica, água morna e mixohalina. A integração de dados faciológicos, estratigráficos e químicos dos depósitos carbonáticos da Formação Pirabas, além de reconstruir o comportamento estratigráfico destas unidades no período estudado, ainda auxiliariam no entendimento das mudanças paleoambientais e paleogeográficas da Plataforma Bragantina e a sua possível relação com os eventos globais

Palavras-chave: Pirita. Carbonato. Neógeno. Plataforma Equatorial. Formação Pirabas.

ABSTRACT

The carbonate-siliciclastic rocks from the early to middle Miocene Pirabas Formation in the equatorial margin of Brazil show a brackish ecofacies of mangrove and coastal lagoons paleoenvironments under tidal influence. The studied section has dark mudstone at the top, characterized by a microbial methanogenesis zone where pyritized trunks, leaves, micro- and macrofossils, and trace fossils, have been investigated. The petrographic characterization and crystallographic analyses distinguish mostly framboids crystal for trunk fragments to the octahedric and cubic crystals from invertebrate shells. The geochemistry analyzes revealed that Fe and S are concentrated both in the fossiliferous content of invertebrate constituents and in the matrix that hosts the trunk, while the other elements are mainly linked to invertebrates. The preferential distribution of these elements is in accordance with the presence of FeS₂ compounds replacing fossils, reflecting the anoxic and reducing conditions of the environment. The pyrite-rich lithostratigraphic section was deposited in a shallow water environment, where pyrite mineralization was developed during the early diagenetic stage under anoxic conditions, plenty of organic matter, warm and mixohaline water. The integration of faciological, stratigraphic and chemical data from the carbonate deposits of the Pirabas Formation, in addition to reconstructing the stratigraphic behavior of these units in the period studied, would also assist in understanding the paleoenvironmental and paleogeographic changes of the Bragantina Platform and its possible relationship with global events.

Keywords: Pyrite. Carbonate. Neogene. Equatorial platform. Pirabas Formation.

LISTA DE ILUSTRAÇÕES

CAPÍTULO 3

Figura 1	Mapa de localização da área de estudo, destacando a localização da Plataforma Bragantina no nordeste do estado do Pará e o posicionamento dos pontos de acesso	06
Figura 2	Contexto tectônico simplificado da margem equatorial norte do Brasil, com destaque para a Plataforma Bragantina. Fonte: Modificado de (Costa <i>et al.</i> 2002, Soares Junior <i>et al.</i> 2008, 2011)	07
Figura 3	Carta litoestratigráfica da Plataforma Bragantina e Pará do nordeste do Estado do Pará, Brasil. Adaptado Rosseti (2013)	10

CAPÍTULO 4

Figura 1	Location map of the study area, highlighting the location of Praia do Atalaia - Salinópolis / PA and the positioning of access points.	16
Figura 2	Facies and Tafofacies of the Pirabas Formation on the outcrop of Praia de Atalaia, Northern Brazil. 1) Fossiliferous trunk; 2) Fragment of partially pyritized wood; 3) Leaf mark registered in fine sediments; 4) Invertebrate mold of pyritized bivalve. Modified Amorim (2016)	17
Figura 3	Taphonomic configuration of the thalassinoid traces: 1 and 2) Tubular morphology with “Y” branch preserved as horizontal endostratic traces allocated in the massive claystone forming a connection network connected to the matrix / sediment and the plant portion; 3) Vegetable filling in the inner portion of the thalassinoids occurring as encrusted with fossil trunks; 4) Internal filling of thalassinoides are composed predominantly of gastropods (E), external molds (A) of internal bivalves (B, C) and bryozoans (D), spine of equinoids (F) ?. (Scale 1, 2 and 3 - 5 cm; 4 - 2 cm	20

- Figura 4 Macroscopic Description: 1) Specimen of gastropods arranged in an oriented manner, with a high degree of abrasion and corrosion, intense fragmentation, low dissolution and partial preservation; 2) Specimen of gastropod arranged in a chaotic manner, reduced degree of abrasion and corrosion, partial fragmentation, low dissolution and partial preservation; 3) Bivalve specimen disposed in an oriented manner in the strata with medium degree of abrasion and corrosion, intense fragmentation, low dissolution and partial preservation; 4) Bivalve specimen arranged in a chaotic manner, allocated perpendicular to the bedding plan, reduced degree of abrasion and corrosion, partial fragmentation, low dissolution and partial preservation; 5 and 6) Specimens of bryozoans arranged in an oriented manner, low degree of abrasion and corrosion, partial fragmentation, low dissolution and high preservation; 7) Fragment of trunk totally pyritized; 8) Trunk fragment without apparent crystallization; 9 and 10) Partly pyritized trunk fractions 22
- Figura 5 Petrographic Description of the Fossils. 1) echinoderm; 2) Briozoa; 3) Green algae; 4) Ostracodes; 5) Ostracode; 6) Foraminifero; 7) Ostracode; 8) Ostracode; 9) Echinoderm; 10) Echinoderm; 11) Briozoa; 12) Ind.?; 13) Bivalve and Foraminiferous; 14) Ostracode; 15) Ind.?..... 25
- Figura 6 Petrographic Description of Fossils. 1) Spine of echinoderm; 2) Ind.?; 3) Ind.?; 4) Ind.?; 5) Ind.?; 6) Gastropod 26
- Figura 7 Crystallographic description of pyrite crystals from SEM analysis. 1) Framboidal pyrite in bivalves, occurring as a filament of euhedral crystals (octahedral and cubic), with size between 5-10 μm (arrow 1), and aggregate of anhedral to subhedral crystals, size between 10-15 μm (arrow 2) ; 2) Euhedral pyrite in gastropods, occurring as octahedral and cubic crystals, well developed, with variable size between 5-20 μm (arrow 1) and overgrowth of amorphous silica crystals (arrow 2); 3) Euhedral pyrite in bryozoans, well-developed crystals, whose size varies between 4-10 μm (arrow 1), as well as overgrowth of apparent amorphous silica crystals (arrow 2); 4) Amorphous Framboidal Pyrite in wood / trunk fragments, variable in size between 4-20 μm (arrow 1); 5) Amorphous Framboidal Pyrite in fragments of wood / trunk with serrated edges or in the form of a "fringe" (arrow); 6) zone filled by pyrite crystals in wood fragments, with cubic shape, and apparent size of 30 μm (arrow 2), amorphous pyrite crystals associated with wood, size 100 μm (arrow 1); 7) Acicular pyrite in leaf impressions, with variable size between 5-50 μm (arrow 1) helically arranged; 8) Acicular pyrite in leaf impressions observed close to the areas of identification of wood fragments (arrow 2) 27

Figura 8	Chemical analysis by EDS. 1 and 2) SEM image of a sample of inverters of gastropods, bivalves and bryozoans showing cubic and orthopedic pyrite crystal with x-ray diffraction crystallogram showing the 2θ peaks of S, Fe, C and O in shot1 and ray diffraction -x showing the 2θ peaks of S, Fe, C and O in shot2	29
Figura 9	Chemical analysis by EDS. 1 and 2) SEM image of a trunk sample showing an amorphous pyrite crystal framboid with x-ray diffraction crystallogram showing the 2θ peaks of S, Fe, Si and O, in addition to Al in shot1 and shot2.	29
Figura 10	Chemical analysis by EDS. 1) SEM image of a trunk sample showing a framboid in amorphous pyrite crystal, with octahedral pyrite filling zones with x-ray diffraction crystallogram showing the 2θ peaks of S, Fe, Si and O, in addition to Al in shot, presence of C in shot3 and high concentrations of S and Fe in Shot4	30
Figura 11	Chemical analysis by EDS. 1) SEM image of leaf sample showing pyrite acicular crystals with x-ray diffraction crystallogram showing the 2θ peaks of S, Ca, O, Fe, K, Na. and Al in shot1; X-ray diffraction crystallogram showing the 2θ peaks of Si, O, Al, S, Fe, Na and Mg in shot2; X-ray diffraction crystallogram showing the 2θ choices of S, Fe, O, Si and Al in shot3	30
Figura 12	X-ray energy dispersion spectrum of invertebrate individuals. The main mineralization (Py and Qtz), corroborates what was highlighted in the analysis by EDS, defining that silicification represents the initial change associated with sulfide	31
Figura 13	X-ray energy dispersion spectrum of invertebrate individuals. In addition to the main mineralization, Marcassita, a polymorph of Pyrite, stands out, highlighting the increase in the pH of the environment or the increase in the temperature of the system	31

SUMÁRIO

DEDICATÓRIA	iv
AGRADECIMENTOS	v
EPIÍGRAFE	vii
RESUMO	viii
ABSTRACT	ix
LISTA DE ILUSTRAÇÕES	x
CAPÍTULO 1	1
1 APRESENTAÇÃO	1
1.1 INTRODUÇÃO	1
1.2 OBJETIVOS	2
1.2.2 Geral	2
1.2.2 Específicos	2
CAPITULO 2	3
2 MATERIAIS E MÉTODOS	3
2.1 ANÁLISE ESTRATIGRÁFICA	3
2.2 ANÁLISE PETROGRÁFICA	3
2.3 MICROSCOPIA ELETRÔNICA DE VARREDURA – MEV	4
2.4 ESPECTROSCOPIA POR ENERGIA DISPERSIVA – EDS	4
2.5 DIFRAÇÃO DE RAIOS - X	4
CAPÍTULO 3	6
3 ÁREA DE ESTUDO	6
3.1 CONTEXTO GEOLÓGICO	7
3.1.1 Compartimentação Tectônica Da Plataforma Bragantina	7
3.1.2 Compartimentação Estratigráfica Da Plataforma Bragantina	8
3.1.2.1 <i>Formação Pirabas</i>	8

CAPÍTULO 4	11
4. ARTIGO 1 - PYRITIZATION IN NEOGENE FOSSIL FLORA AND FAUNA FROM MANGROVE-COASTAL LAGOONS AT THE PIRABAS FM, BRAZIL	
4.1 INTRODUCTION	12
4.2 METHODS	13
4.3 GEOLOGICAL SETTINGS	14
4.3.1 Stratigraphy	16
4.3.2 General aspects of the fossiliferous assemblage	18
<i>4.3.2.1 Fauna</i>	18
4.3.2.1.1 Gastropods	18
4.3.2.1.2 Bivalves	18
4.3.2.1.3 Bryozoan	19
4.3.2.1.4 Thalassinoides Technofossil	19
<i>4.3.2.2 Flora</i>	20
4.3.2.2.1 Trunks	20
4.3.2.2.2 Leaves	21
4.4 PETROGRAPHY AND GEOCHEMISTRY	23
4.4.1 Petrography setting	23
4.4.2 Depositional constituents	24
4.4.3 Crystallography setting	26
4.4.4 Elemental geochemistry	28
4.4.5 X-ray diffractometry (DRX)	31
4.5 DISCUSSIONS	31
4.6 DIAGENESIS	37
4.7 CONCLUSION	38
CAPÍTULO 5	46
5.1 CONSIDERAÇÕES FINAIS	46
REFERÊNCIAS	47

CAPÍTULO 1

1 APRESENTAÇÃO

1.1 INTRODUÇÃO

A Formação Pirabas aflora em falésias na zona litorânea dos estados do Maranhão, Piauí e Pará, e é caracterizada por rochas carbonáticas e argilitos de idade Oligo-Miocena (Maury 1925, Petri 1957, Ferreira 1966, 1982, Fernandes 1984), recobertas por depósitos miocenos siliciclásticos da Formação Barreiras (Rossetti *et al.* 2001), ambos sobrepostos, discordantemente, pelos sedimentos Pós-Barreiras (Góes *et al.* 1990). O embasamento é composto por rochas ígneas e metamórficas pré-cambrianas (Klein & Moura 2003), assim como depósitos siliciclásticos paleozoicos do Arenito do Guamá e do Grupo Itapecuru (Rossetti & Góes 2004).

Os constituintes fósseis, do Mioceno (23 -5.3 Ma) da Plataforma Bragantina no norte do Brasil é marcado por depósitos carbonáticos ricamente fóssilíferos pertencentes a Formação Pirabas. Os trabalhos paleontológicos considerados referências históricas para a descrição da fauna e flora desta unidade são os de White (1887) e Maury (1925) para moluscos, briozoários e corais; as contribuições de Petri (1957) para foraminíferos, Beurlen (1958) para crustáceos, Santos (1958, 1967) em equinoides, Santos & Travassos (1960) em peixes, Paula-Couto (1967) nos sirenídeos e o de Duarte (2004) na paleoflorula. Referências mais recentes sobre registros de diferentes táxons fósseis estão em Távora *et al.* (2007), Aguilera e Paes (2012), Aguilera *et al.* (2013, 2017a,b), taxonomia de briozoários (Ramalho *et al.* 2015, 2017, Muricy *et al.* 2016) e a taxonomia e bioestratigrafia de ostracodes (Nogueira & Nogueira 2017).

Apesar dos relevantes estudos desenvolvidos pelos diferentes autores anteriormente citados a problemática que envolve a região está relacionada a carência de dados referentes aos processos diagenéticos baseados no grau de sulfetação (piritização) e oxidação dos diferentes níveis estratigráficos presentes na Formação Pirabas, uma vez que a formação de pirita sedimentar durante a diagênese inicial é um processo importante para controlar o nível de oxigênio da atmosfera e a concentração de sulfato na água do mar ao longo do tempo geológico (Berner 1991). A quantidade de pirita que pode se formar em um sedimento é limitada pelas taxas de fornecimento de matéria orgânica decomponível, sulfato dissolvido e minerais de ferro detrítico reativos. A matéria orgânica parece ser o principal controle na formação de pirita em sedimentos marinhos terrígenos normais (não euxínicos), onde o sulfato dissolvido e os minerais de ferro são abundantes. Em contrapartida, a formação de pirita em sedimentos de

água doce não marinhos é severamente limitada por baixas concentrações de sulfato e esta característica pode ser usada para distinguir xistos de água doce de xistos marinhos ricos em espécies orgânicas antigas (Moreira *et al.* 2018).

Desta forma, a integração de dados faciológicos, estratigráficos e químicos dos depósitos carbonáticos da Formação Pirabas, além de reconstruir o comportamento estratigráfico destas unidades no período estudado, ainda auxiliariam no entendimento das mudanças paleoambientais e paleogeográficas da Plataforma Bragantina e a sua relação com os eventos globais. Os dados aqui apresentados têm por finalidade expandir o conhecimento a respeito dos processos diagenéticos (eodiagênese) de idade Oligo-mioceno, situada na zona costeira da Plataforma Bragantina, de onde foram coletadas amostras de níveis distintos, próximo a zona de contato com a Formação Barreiras, utilizando para isso ferramentas multidisciplinares, tais como a Análise Mineralógica, Petrografia Ssdimentar, Microscopia Eletrônica de Varredura (MEV-EDS) e Difração de Raio X (DRX). Sendo assim, esse trabalho pretende disponibilizar uma base de dados nova para as discussões sobre os níveis piritizados de idade Oligo-mioceno com a finalidade de expandir o conhecimento a respeito da dinâmica palwoambiental e geoquímica no período destacado.

1.2 OBJETIVO

1.2.1 Geral

O objetivo principal desta pesquisa é reconstituir o paleoambiente característico dos fósseis piritizados da Formação Pirabas bem como estruturar a evolução ambiental através da reconstrução diagenética do material e da área estudados.

1.2.2 Objetivos Específicos

- Destacar os paleoambientes deposicionais;
- Descrever as assembleias fossilíferas piritizadas;
- Determinar a estrutura morfológica dos diferentes níveis piritizados;
- Correlacionar as assembleias fossilíferas piritizadas e o ambiente deposicional;

CAPÍTULO 2

2 MATERIAIS E MÉTODOS

Para a elaboração deste trabalho foram realizados trabalhos de campo e laboratoriais de modo que os materiais fossilífero foram previamente analisados, descritos, fotografados e posteriormente coletados. Durante as atividades de campo, as análises foram feitas ao longo de um perfil estratigráfico remontado sobre quadrículas de espaçamento 2x2m, de modo que se pudesse obter um número qualitativo e quantitativo de litologia, estrutura e espécime fóssil. Sendo assim, foram coletadas, para posterior análise laboratorial 32 amostras macroscópicas, entre rocha matriz e fósseis, estes por sua vez foram armazenados no Laboratório de Geologia Sedimentar da Universidade Federal do Pará – UFPA. Posteriormente, o material selecionado foi triado e direcionado para as análises laboratoriais realizadas na própria UFPA, petrografia, microscopia eletrônica de varredura, espectroscopia por energia dispersiva e difração de raio-x.

2.1 ANÁLISE ESTRATIGRÁFICA

A determinação acerca do comportamento estratigráfico dos depósitos carbonáticos pertencentes à unidade Pirabas foi realizada seguindo o modelo proposto por Read (1982) definido a partir das litologias, assembleias fossilíferas e arranjo tafonômico. O mapeamento da distribuição horizontal e vertical destas fácies foi auxiliado por perfis verticais, bem como a construção de seções esquemáticas e panorâmicas obtidas a partir do enquadramento do afloramento, seguindo a formação de quadrículas com espaçamento (2x2m).

2.2 ANÁLISE PETROGRÁFICA

Para análise petrográfica, foram confeccionadas no laboratório de laminação da Universidade Federal do Pará – UFPA 5 (cinco) lâminas delgadas, com o intuito de observar, petrograficamente, a relação da matriz com os componentes aloquímicos, especificamente os bioclastos, e os terrígenos presentes. A classificação das fácies, e sua interpretação ambiental foram baseadas nos aspectos texturais, arcabouço estratigráfico, presença de bioclastos, quantidade de grãos, estruturas internas e bioturbação (Dunham 1962, Embry & Klovan 1971, Tucker 1992).

2.3 MICROSCOPIA ELETRÔNICA DE VARREDURA - MEV

O Microscópio Eletrônico de Varredura LEO-ZEISS modelo 1430, do Laboratório de Microscopia Eletrônica de Varredura - LABMEV da Universidade Federal do Pará (UFPA) foi utilizado para obtenção de imagens de elétrons retroespalhados da matriz, dos constituintes fósseis invertebrados (bivalves e gastrópodes) e do material vegetal (tronco e fragmento de madeira) pertencentes a Formação Pirabas. A análise teve como objetivo observar, microscopicamente, a morfologia e a estrutura dos principais núcleos piritizados identificados tanto no conteúdo fossilífero, quanto no material vegetal. As amostras foram metalizadas com ouro e o tempo de recobrimento foi de 1,5 minutos. As condições de operação para o imageamento em elétrons secundários foram: corrente do feixe de elétrons = 90 μA , voltagem de aceleração constante = 10 kv, distância de trabalho = 15 mm.

2.4 ESPECTROSCOPIA POR ENERGIA DISPERSIVA - EDS

A espectroscopia por energia dispersiva (EDS) é baseada, na maioria dos casos, selecionando uma área da superfície da amostra obtendo-se uma imagem bidimensional, varrendo uma área que varia de cerca de 1 cm a 5 μm utilizando técnicas de “*Scanning Electron Microscopy*” (SEM) cuja ampliação pode variar de 20 vezes à 30.000 vezes com resolução espacial de cerca de 50 à 100 nm. É na análise local de algum ponto que se pode fazer alguma aferição qualitativa ou semi-quantitativa na composição química usando EDS. A energia de entrada dos raios-X é absorvida por um detector de EDS no qual contém um cristal e esse feito se dá por ionização que gera elétrons livres no cristal através da produção de corrente de carga elétrica. Assim, tem-se a energia dos raios-X convertidos em tensão elétrica, no qual tais pulsos correspondem aos raios-X característicos do elemento (Severin 2004). A análise teve como objetivo destacar os diferentes elementos químicos presentes e predominantes em pontos selecionados a partir da análise do MEV, realizada no laboratório da Universidade Federal do Pará (UFPA).

2.5 DIFRAÇÃO DE RAIOS-X

As análises por DRX foram realizadas no Difrátômetro de Raios-X (DXR) modelo Empyrean da PANalytical, tubos de raios-X cerâmico de anodo de Co ($K_{\alpha 1} = 1,789010 \text{ \AA}$), foco fino longo, filtro K_{β} de Fe, detector PIXCEL3D-Medpix3 1x1, no modo *scanning*, com voltagem de 40 kV, corrente de 35mA, tamanho do passo $0,0263^{\circ}$ em 2θ , varredura de $3,0072^{\circ}$ a $94,9979^{\circ}$ em 2θ , tempo/passo de 30,6s, fenda divergente: $1/4^{\circ}$ e anti-espalhamento: $1/2^{\circ}$, máscara: 10 mm, pertencente ao laboratório da Universidade Federal do Pará (UFPA). A análise

por Difração de Raios-X (DRX) possibilitou a caracterização e quantificação da mineralogia principal e secundária que ocorre na matriz carbonática que abriga os níveis piritizados. A preparação consiste da pulverização em grau de ágata para posterior preenchimento em porta amostra específico para a análise, pelo método de *back-loading*, que evita sensivelmente o efeito de orientação preferencial.

CAPÍTULO 3

3 ÁREA DE ESTUDO

A área de estudo encontra-se localizada na região norte do Brasil (fig. 1), nordeste do Estado do Pará, abrigando o município de Salinópolis/PA, cujas coordenadas geográficas são $0^{\circ} 36'5''\text{S}$ e $47^{\circ}18' 4''$, à cerca de 214 km da cidade de Belém. Foram visitados 5 (cinco) afloramentos durante 3 (três) dias de atividades de campo, sendo mais relevante para o presente trabalho o afloramento localizado na Praia do Atalaia, caracterizado, principalmente, por falésia ao longo da linha de costa da praia.

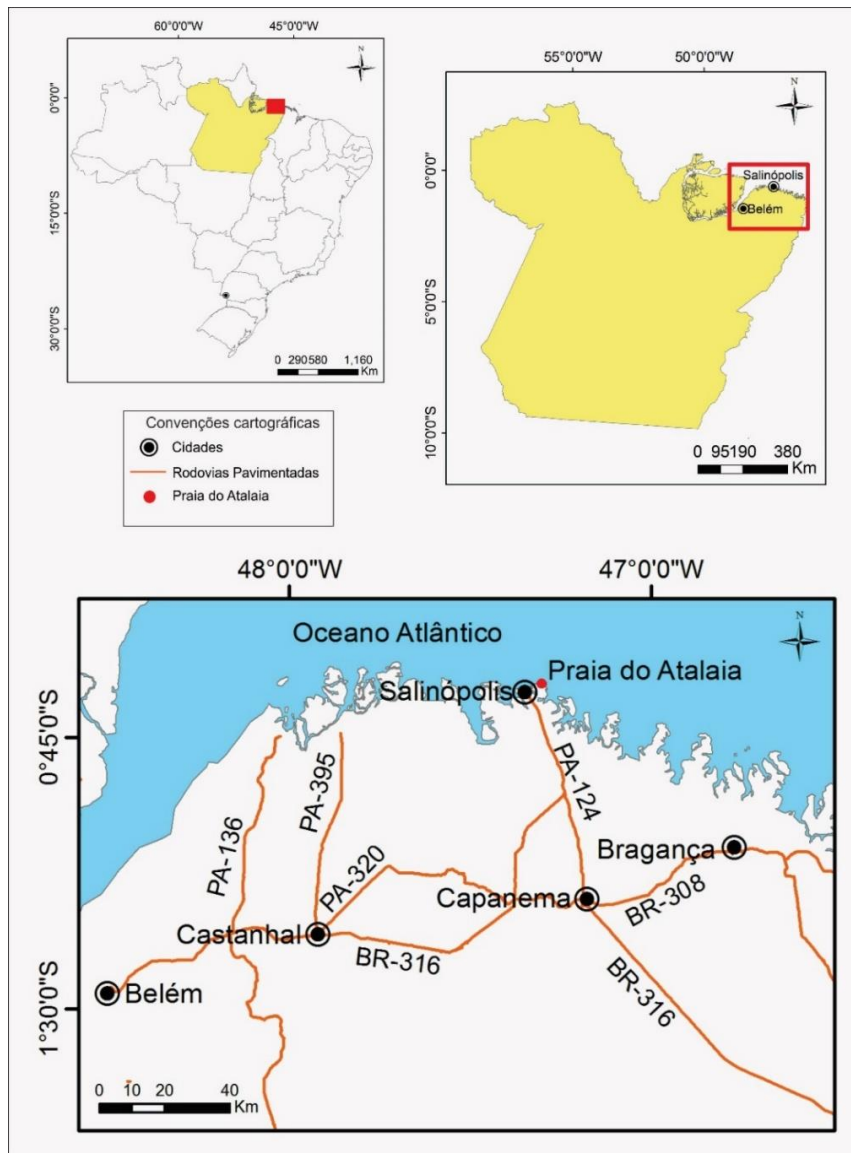


Figura 1- Mapa de localização da área de estudo, destacando a localização da Praia do Atalaia – Salinópolis/PA e o posicionamento dos pontos de acesso.

3.1 CONTEXTO GEOLÓGICO

3.1.1 Compartimentação tectônica da plataforma bragantina

A Plataforma Bragantina aflora, em grande parte, na porção nordeste do estado do Pará, e corresponde a duas áreas planas, segmentadas pela Fossa Vigia-Castanhal (Klein & Moura 2003, Rossetti & Góes 2004). O embasamento desta plataforma é composto por rochas ígneas e metamórficas, assim como arenitos paleozoicos na região de São Miguel do Guamá (Klein & Moura 2003, Rossetti & Góes 2004). Na transição Oligo-Mioceno, o regime de tectônica intraplaca passou a atuar de forma predominante na região equatorial norte do Brasil, marcado por sistemas transcorrentes, cujas estruturas principais apresentavam direção NE-SW e transectadas por falhas normais E-W e NW-SE. (Costa *et al.* 2002, Soares Junior *et al.* 2011).

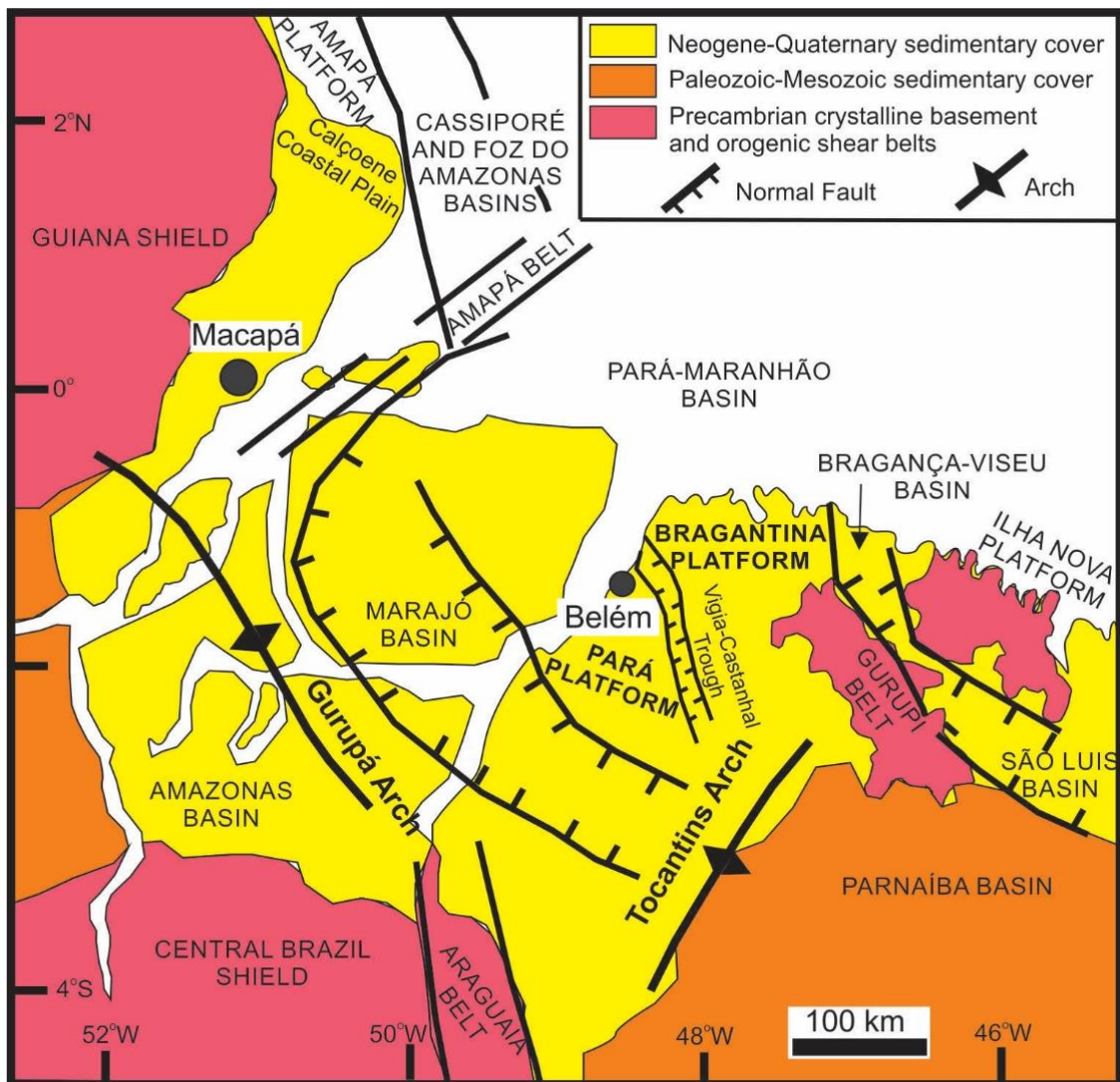


Figura 2- Contexto tectônico simplificado da margem equatorial norte do Brasil, com destaque para a Plataforma Bragantina. Fonte: Modificado de (Costa *et al.* 2002, Soares Junior *et al.* 2008, 2011).

Na Plataforma Bragantina a tectônica também apresentava essa mesma orientação, cuja tectônica era marcada por sistemas transcorrentes dextrais associados a dois pulsos de inversão (transpressão e transtensão) da Bacia de Grajaú (Costa *et al.* 1996, Soares Jr. *et al.* 2011). Esse evento gerou subsidência de blocos tectônicos e formação de grabens e semigrabens orientados na direção NW-SE, que se estabeleceram de forma concomitante aos eventos transgressivos do Mioceno, favorecendo a deposição de carbonatos marinhos da Formação Pirabas até 150 km ao sul do continente (Costa *et al.* 1996, 2002, Rossetti & Góes 2004, Soares Jr. *et al.* 2011). O desenvolvimento deste cenário foi essencial para a preservação do registro sedimentar da Plataforma Bragantina, uma vez que, o conjunto de reativações tectônicas causaram sucessivos rearranjos de leitos de rios e deslocamentos de blocos do embasamento da plataforma, favorecendo a entrada do mar a grandes distâncias nas áreas continentais e a deposição das rochas carbonáticas da Formação Pirabas (Costa *et al.* 1996, Soares Jr. *et al.* 2011).

3.1.2 Compartimentação estratigráfica da plataforma bragantina

As formações Pirabas, Barreiras e sedimentos Pós-Barreiras são as unidades litoestratigráficas que ocorrem na Plataforma Bragantina. A deposição dessas formações teve início no final do Oligoceno e foi influenciada por variações eustáticas globais e reativações tectônicas regionais (Costa *et al.* 1996, Rossetti *et al.* 2013) (fig. 2).

3.1.2.1 Formação Pirabas

A Formação Pirabas (fig.3), datada do Mioceno inferior, segundo Maury (1925), ocorre descontinuamente nas regiões norte e nordeste, nos estados do Pará, Maranhão e Piauí. Geologicamente, as estruturas que controlaram a deposição da Formação Pirabas, influenciadas por movimento tectônico, são falhas normais NW-SE e inclinadas para NE, e falhas transcorrentes NE-SW que funcionaram como zonas de transferência.

Segundo Rossetti & Góes (2004) não existe estudo prévio documentando as microfácies carbonáticas miocênicas correspondentes à Formação Pirabas. No geral, uma análise microscópica revela domínio de *wackestones* e *rudstones*, composto por *floatstones* e *mudstones*, embora presentes em menor frequência. Estas rochas apresentam o arcabouço aberto, sustentado por lama micrítica e com grãos flutuantes que atestam ausência de processos de compactação. Desde sua formalização como unidade litoestratigráfica, os sedimentos da Formação Pirabas são considerados como miocênicos. Entretanto, Ferreira *et al.* (1981) classificou sua deposição como oligocênica a miocênica, baseado na correlação com pacotes

sedimentares da Bacia da Foz do rio Amazonas, assim como pela presença do gastrópode *Orthaulax Pugnax* e foraminífero planctônico *Globorotalia Opima Bolli*.

Datações baseadas em foraminíferos planctônicos e bentônicos (Távora & Fernandes, 1999), moluscos bivalves (Fernandes & Távora, 1990), palinórfos (Leite *et al.* 1997a, b) e ostracodes (Nogueira *et al.* 2013) indicaram uma idade Mioceno Inferior, com base nos resultados em estudos taxonômicos e bioestratigráficos que envolveram a identificação de mais de 100 espécies ostracodes na sucessão Pirabas, atestaram idade Oligoceno-Mioceno para estes depósitos (Nogueira 2015). Aguilera & Paes (2012) e Aguilera *et al.* (2013) sugerem que esta heterogeneidade na sedimentologia e paleontologia, e conseqüentemente, nos paleoambientes associados, poderiam suportar uma divisão formal ou informal em diferentes membros e/ou indicar diferentes idades ao longo da sequência da Formação Pirabas.

Segundo Góes *et al.* (1990) o arranjo dos depósitos da Formação Pirabas evidencia padrão geral prográdacional, revelado pela superposição de fácies de plataforma aberta por fácies progressivamente mais costeiras, associadas a sistema deposicional contendo ilhas-barreiras. Dados mais concretos indicam que Formação Pirabas se depositou em um ambiente de plataforma rasa, constituídos por subambientes de laguna, *shoreface/foreshore* e depósitos de mangue/lama (Góes *et al.* 1990, Rossetti & Góes 2004, Rossetti *et al.* 2013). Segundo Góes *et al.* (1990), embora a organização das fácies registre eventos transgressivos ocorridos durante o Mioceno, a distribuição de arquitetura estratal indica um padrão prográdacional. Isto é revelado pela superposição de plataforma interna com ambientes progressivamente costeiros, que resultou no aumento de influxos siliciclásticos.

O estudo dos eventos biológicos, como a criação ou mudança nos biótopos e ecossistemas, aparecimento ou desaparecimento de grupos de organismos estão intimamente relacionados com os processos geológicos e propiciaram colonização ou substituição dos indivíduos das comunidades. Dentre estes, os gastrópodes são de longe os mais abundantes, com o recorde compreendendo cerca de 324 espécies (Távora *et al.* 2004). Microfósseis também são abundantes, e consistem principalmente em foraminífritos bentônicos e planctônicos, ostracodes e, em menor escala, nanofósseis (Ramos *et al.* 2004). Os vertebrados são na sua maioria marinhos e incluem cavalos marinhos, peixes ósseos, tubarões e raias, com ocorrências locais de répteis (Costa *et al.* 2004). Os grãos de pólen correspondem principalmente a 91 espécies de angiospermas, com esporos de pteridófitos e briófitos subordinados (Leite 2004). A paleoflora descrita na Formação Pirabas é representada por folhas bem preservadas de 19 gêneros pertencentes a 18 famílias de angiospermas (Duarte 2004).

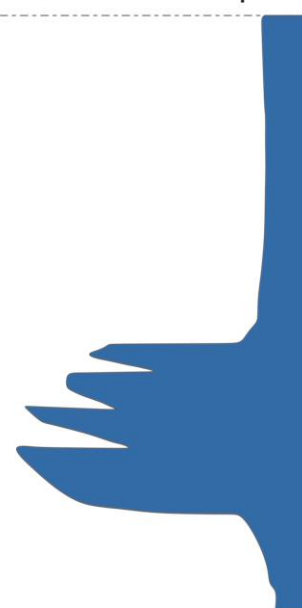
IDADE	SEQUÊNCIA DEPOSICIONAL	UNIDADE LITOESTRATIGRÁFICA	NÍVEL DO MAR	
			← Alto	Baixo →
Pli-Pleistoceno	C	Pós-Barreiras	?	?
MIOCENO	NEO	Paleossolo laterítico		
		B		Formação Barreiras
	MESO	A		Formação Barreiras
Formação Pirabas				
Neo Oligoceno				
Paleogeno		Paleossolo laterítico		
Cretáceo		Grupo Itapecuru		

Figura 3- Carta litoestratigráfica da Plataforma Bragantina e Pará do nordeste do Estado do Pará, Brasil. Modificado Rosseti (2013).

CAPÍTULO 4

PYRITIZATION IN NEOGENE FOSSIL FLORA AND FAUNA FROM MANGROVE-COASTAL LAGOONS AT THE PIRABAS FM, BRAZIL

Giovanni A. T. Da Mata¹, Orangel Aguilera^{2*}

¹Federal University of Para (UFPA), Geoscience Institute, Rua Augusto Corrêa, s/n, CEP 66075-110, Belém, Pará, Brazil. damata.giovanni@yahoo.com.br; ²Fluminense Federal University (UFF), Paleocology and Global Changes Laboratory, Rua Marcos Waldemar de Freitas Reis, S/no, Campus Gragoatá, Bloco M, Lab. 110, CEP. 24210-201, Niterói, Rio de Janeiro, Brazil.

Abstract

The carbonate-siliciclastic rocks from the early to middle Miocene Pirabas Formation in the equatorial margin of Brazil show a brackish ecofacies of mangrove and coastal lagoons paleoenvironments under tidal influence. The studied section has dark mudstone at the top, characterized by a microbial methanogenesis zone where pyritized trunks, leaves, micro- and macrofossils, and trace fossils, have been investigated. The petrographic characterization and crystallographic analyses distinguish mostly framboids crystal for trunk fragments to the octahedric and cubic crystals from invertebrate shells. The geochemistry analyzes revealed that Fe and S are concentrated both in the fossiliferous content of invertebrate constituents and in the matrix that hosts the trunk, while the other elements are mainly linked to invertebrates. The preferential distribution of these elements is in accordance with the presence of FeS₂ compounds replacing fossils, reflecting the anoxic and reducing conditions of the environment. The pyrite-rich lithostratigraphic section was deposited in a shallow water environment, where pyrite mineralization was developed during the early diagenetic stage under anoxic conditions, plenty of organic matter, warm and mixohaline water.

Keywords: Pyrite mineralization. Carbonate. Neogene. Equatorial platform. framboids crystal.

Highlights

The main objective of this research is structured in the characterization of the pyritized fossils of the Pirabas Formation as well as tracing the diagenesis of the highlighted content as follows:

- Paleomangrove organic-rich sediments at the redox zone are enriched in syngenetic and diagenetic pyrite
- Pyritized flora and faunal were an important component of coastal lagoon and mangrove paleoenvironment
- Framboidal pyrite euhedral crystals in shell and tests differ from framboids amorph and acicular crystal in trunk and leaves
- Pyritic burrow fills in the mudstone matrix was favorable by the concentration of sulfide ions in early diagenesis

4.1 INTRODUCTION

Authigenesis of pyrite (FeS_2) occurs mainly in deep subaqueous and oxic-dysoxic environment conditions, both in continental and marine settings, commonly as disseminated minerals in low permeability black shale (Jorgensen 1977). Pyrite can also be developed in shallow environments, composing the matrix of organic matter-rich sediments, or replacing fossils, especially in the presence of sulfate-reducing bacteria (Briggs *et al.* 2003). This anoxic conditions can be achieved in mangrove and coastal settings, caused mainly by the interplay of high contents of labile iron, sulfide, and organic matter linked to brackish water geochemistry and proliferation of sulfate reducing organisms (Scholz & Neumann 2007, Álvarez-Iglesias & Rubio 2012, Tripathi *et al.* 2015). A great opportunity to address this issue is provided by the Pirabas Formation, in northern Brazil. This succession represents a mixed carbonate-siliciclastic that is possibly associated with the final stages of an abrupt episode of global cooling at the Oligocene-Miocene boundary, the Mi-1 glaciation (Egger *et al.* 2018), and the global warming period of the middle Miocene climate maximum (Goldner *et al.* 2014), in a coastal equatorial platform that predated the Amazon delta (Figueiredo *et al.* 2009, Watts *et al.* 2009, Aguilera *et al.* 2020). These deposits portray a continuum littoral system, including foreshore/shoreface, marginal lagoons, restricted platforms, and mangrove estuarine lagoons laterally and vertically connected (Rossetti *et al.* 2013 and references therein).

This work presents new data regarding the understanding of the factors involved in the pervasive and uncommon pyritization zone involved heterozoan carbonate framework across equatorial Miocene coastal settings. The redox transition zone from the Atalaia outcrop, upper

part of the Pirabas Formation, including anaerobic or aerobic bacterial leaching nitrate-dependent responsible for pyrite oxidation of insoluble metal sulfides, under acidic-pH (Sandrs *et al.* 1995, Percak-Dennett *et al.* 2017). The pathways of biological or chemical pyritization processes were discussed at length in Jorgense *et al.* (2019) and Renac *et al.* (2020). The pyrite oxidize zone previously recorded at the middle section of Atalaia outcrop by Aguilera *et al.* (2020) has almost 50 cm depth; however, new outcrops in the Atalaia section showed an exhumed zone, overlapped by the Barreira Formation, and this exhumed zone is studied here. This surficial record at the top of the section is in agreement with the literature as pyritized zone could be recorded at meters to tens of meters below the land surface (Gu *et al.* 2020). The pyrite from the Atalaia redox zone has completely oxidized all fossil contents throughout the layer and during pseudomorphism, the pyrite iron oxides replace iron sulfide while retaining the external shape exemplified by octahedral Fe oxide microcrystals within framboids in agreement with the description of Gu *et al.* (2020).

4.2 METHODS

Field trips to the Pirabas Formation were conducted in May 2108, at the Atalaia Beach outcrop (Fig. 1), Salinópolis municipality, Pará State, northern Brazil. We followed the referential stratigraphic section at Atalaia (e.g., Aguilera *et al.* 2017, 2020) to recognize the zone with pyritized fossils and collect the samples. The location seems to be at the very top of the entire Atalaia outcrop, just below the contact with the overlying Barreiras Formation. Plant fossils (trunks and leaves) samples, and invertebrate specimens were photographed *in situ* and collected for petrography and geochemistry analyses.

Five thin petrographic slides were prepared for analysis, fixed to 76 × 26 mm glass slices, and polished to 30 µm thick. The petrographic analyse following the classification of Folk (1964) through the ribbon counting technique (300 points by each thin section) (Galehouse 1971). Specimens and petrographic slides were deposited at the Laboratory of Sedimentology in the Federal University of Pará (UFPA) under the catalog numbers: FP-01, FP-02, FP-03, FP-04, and FP-05. The photomicrographs were obtained using a petrographic microscope ZEISS. The scanning electron microscopy (SEM) imaging of samples was obtained at LABMEV-UFPA using an LEO-ZEISS electronic microscope model 1430. The samples were mounted on aluminum supports, 12 mm in diameter, using double-sided carbon adhesive tape. The thin sections were metalized with Au for one minute and five seconds, resulting in a gold film with an average thickness of 12 nm. Images were generated during the secondary electron detection, using an acceleration voltage of 10 kV, and working on the distance of approximately 15 mm.

At the same time, the most abundant chemistry elements from individual shots were identified using stereoscopy disperses energy (SDE). Several shots were taken on invertebrates, trunk, and leave fossils.

Whole-rock geochemical analyses and mineral characterization was conducted in the Laboratory of Geochemistry (UFPA). The first step of pulverized samples was carried on the mortar. The data were obtained through an X-ray diffractometer, PANALYTICAL X'PERT PRO MPD (PW 3040/60), with an X-ray tube and ceramic anode Cu ($K\alpha_1 = 1,789010 \text{ \AA}$), filter $K\beta$ of Fe, detector PIXCEL3D-Medpix3 1x1. The following analytical parameters were utilized: voltage of 40 kV, amperage of 35 mA, step size 0.0263° , time per step 30.6s, a divergent slit of $1/2^\circ$, mask fixed at 10 mm, and scanning of 3.0072° to 94.9979 in 2θ . The data acquisition was performed with the X'Pert Data Collector software and processed with X Pert High Score software, version 2.1b. The qualitative elementary geochemistry analyses (Al, C, Fe, K, Mg, Na, O, S, Si) were conducted using energy dispersion x-ray spectrometry (EDS). EDS shots sampling were made in selected regions of crystallographic MEV images that have distinct morpho-textural patterns between flora (for example, logs, wood fragments, and leaves) and fauna (for example, gastropods, bivalves and bryozoans). Two EDS-shots were taken at the amorphous pyrite crystals in the trunk, four EDS-shots at the wood fragments in the amorphous and octahedral pyrite crystals, and three EDS-shots at the taped-shape and needle-shaped crystal in leaves. The mineral identification was performed using the standard comparative diffractogram form of Inter Center for Diffraction Data e Powder Diffraction File) (ICDD-PDF).

4.3 GEOLOGICAL SETTING

The Pirabas Formation is part of the Bragantina Platform, a sedimentary succession that overlies the metasedimentary basement rocks of Northern Brazil, and considered an onshore extension of the Pará-Maranhão Basin (Rossetti & Góes 2004, Rossetti *et al.* 2013). The mixed siliciclastic-carbonate Pirabas Formation (early-middle Miocene) was deposited in a complex system of interconnected shallow-water coastal environments, developed on a wide and gently sloping shelf (Rossetti *et al.* 2013, Aguilera *et al.* 2020a, b). The various facies of the Pirabas Formation have been grouped into three major ecofacies: 1) the Capanema Ecofacies (related to the lagoonal environment); 2) the Baunilha Grande Ecofacies (related to open marine, lagoon, and mangrove forest environment); and 3) the Castelo Ecofacies (related to a carbonate platform environment) (Antonioli *et al.* 2015 and references therein). However, the Atalaia outcrop ecofacies is a mixture of paleoenvironmental dynamics overlapping the diagnosis

attribute to Baunilha Grande Ecofacies and Castello Ecofacies. As in the modern Northern Brazilian Shelf, the Pirabas shelf was dominated by siliciclastic sediments in coastal areas, whereas carbonate production was more relevant in areas far off the coast (Aguilera *et al.* 2020b).

The outcrop at the Atalaia Beach comprises an up to 8 m-thick section that includes lithotypes of the Pirabas Formation (5 m-thick) overlapping by the Barreiras Formation (3 m-thick) in an abrupt contact between carbonates and siliciclastic rocks, respectively, whose geographical coordinates are 0 ° 36'5 "S and 47 ° 18 '4, about 214 km from the city of Belém (fig. 1).

The Atalaia outcrops show a dynamic of environmental successions along the sections where the framework are characterized by the following microfacies: (1) shallow-water inshore platform, (2) brackish, and (3) surf zone (Aguilera *et al.* 2020). The mixture of siliciclastics and bioclasts on lithified packstones, friable wackestone, and mudstones were reflected in the sedimentary processes through the section.

Calcareous algae, sporomorphs of angiospermas, and pteridophytes, represented the paleoflora from the Atalaia deposits with a highlight in common species of mangrove. On the other hand, the faunal assemblages include foraminifera, ostracods, sponges, bryozoans, ahermatypic corals (non-reef-building), mollusks, echinoderms, crustaceans, fish, and sirenids mammals that seem to have accumulated in shallow tropical marine palaeoenvironment (Appendix 1 and references therein).

The microfacie attribute to the lagoon and mangrove forest environment from the Pirabas Formation show pyritization processes (Ferreira *et al.* 1981, Antonioli *et al.* 2015, Aguilera *et al.* 2020a, b, Araújo *et al.* in press) mostly related with the black mudstone in the section.

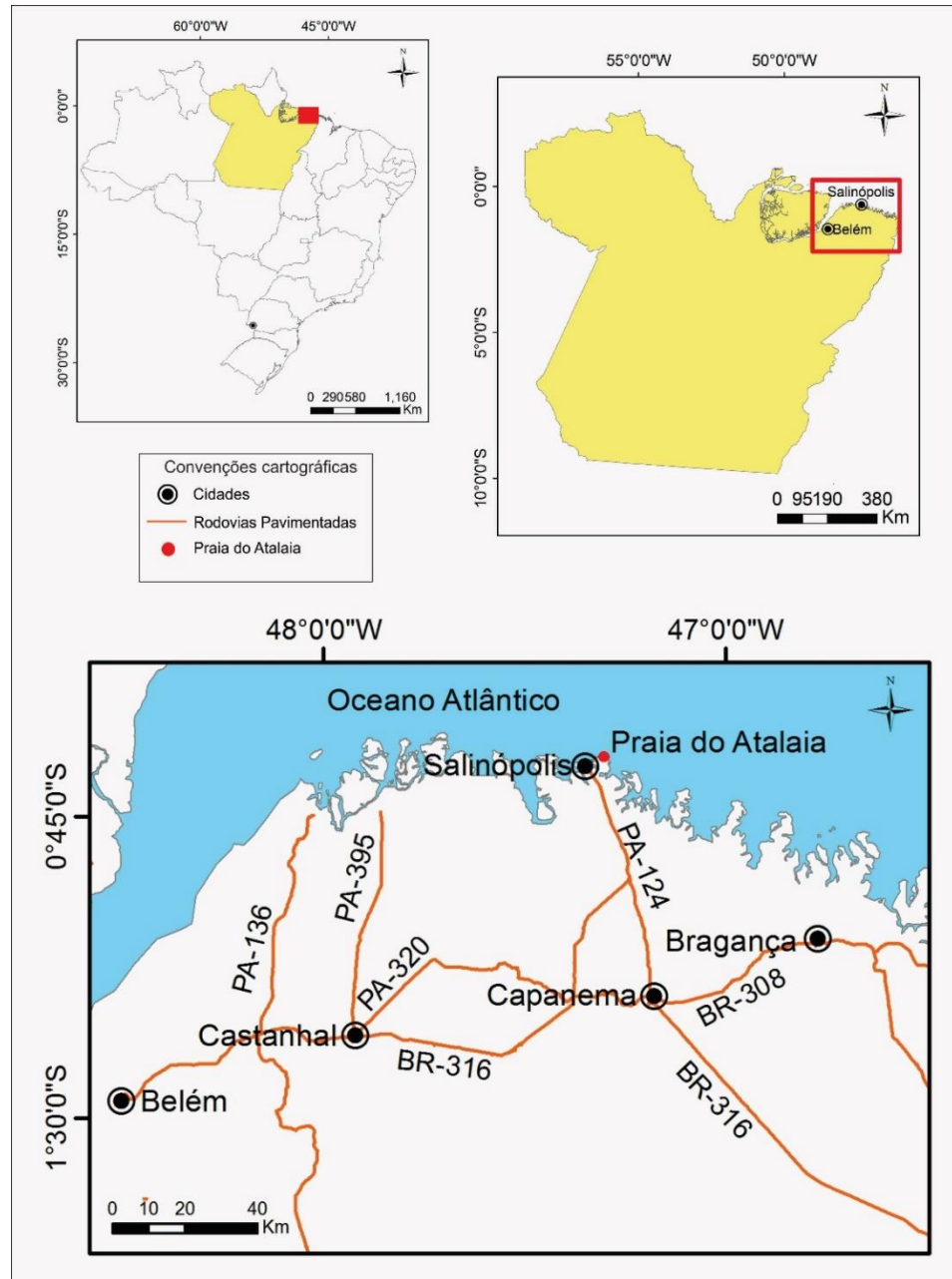


Figure 1 - Location map of the study area, highlighting the location of Praia do Atalaia - Salinópolis / PA and the positioning of access points.

4.3.1 Stratigraphy

The Atalaia outcrop comprises an up to 8 m-thick section (fig.2) that includes lithotypes from the Pirabas and Barreiras formations, represented by an abrupt contact between carbonates and siliciclastic rocks, respectively. The first 5 meters are attributed to the Pirabas Formation constituted of biocalcirudite, non-stratified biocalcarenite, stratified biocalcarenite, marl, biohermite, calcilutite and organic matter-rich mudstones (Góes *et al.* 1990). These are tabular to irregular beds, locally including shale lenses.

The fossiliferous assemblage of the Atalaia outcrop comprises abundant biota with macrofossils and microfossils, and flora (Aguillera *et al.* 2020). The highest faunal content and diversity occur in closed-packed and massive biocalcirudites, including individuals that are whole or fragmented, with different ontogenetic stages. The bioclasts comprise invertebrate organisms, such as foraminifera, echinoderms, coelenterates, pelecypods, bryozoans, crustaceans, ostracods, cephalopods, and vertebrates. Structureless biocalcarenite presents scattered individuals, with low diversity, as well as plant fragments and clay clasts that occur as lag deposits in the basal portion of the beds. Cross-bedded biocalcarenites exhibit low to medium-scale hummocky cross-stratifications and heterolithic bedding, varying from flaser to lenticular bedding upsection. Allochemical constituents in these strata include fragmented fossils composing a closely-packed framework. The overlying marl beds are up to 8 m-thick in correlatable outcrops (Capanema section) and characterized by even-parallel laminations with high bioturbation index. The massive mudstone facies exhibits a sharp lateral passage between green and black-colored beds, with plentiful pyritized fauna and plant fossils (the focus of this study) representative of a coastal setting with mangrove forest (Góes *et al.* 1990, Aguilera *et al.* 2020).

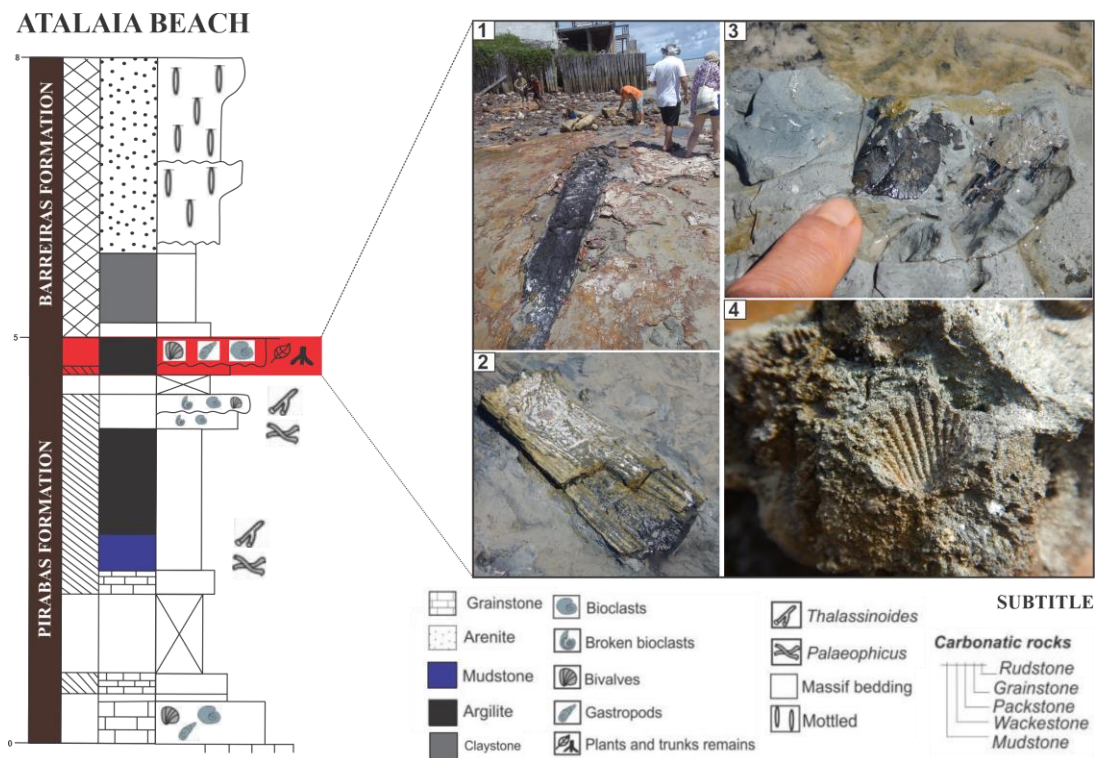


Figure 2 - Facies and Tafofacies of the Pirabas Formation on the outcrop of Praia de Atalaia, Northern Brazil. 1) Fossiliferous trunk; 2) Fragment of partially pyritized wood; 3) Leaf mark registered in fine sediments; 4) Invertebrate mold of pyritized bivalve. Modified Amorim (2016).

4.3.2 General aspects of the fossiliferous assemblage

The fossiliferous assembly present in the study area presents diversity and is arranged in a predominantly chaotic manner. This assembly is composed of gastropods, bivalves, bryozoans, ostracodes and echinoderms, in addition to fossil traces of the genus *Thalassinoides*. The present flora includes trunks oriented parallel to the host rocks, in addition to fragments of trunks and leaf impressions randomly arranged.

4.3.2.1 Fauna

4.3.2.1.1 Gastropods

Specimens of gastropods have distinct distributions and are divided into two groups. A group arranged in the strata (fig. 4.1), with taphonomic signature characterized by a high degree of abrasion and corrosion, reduced fragmentation and low degree of dissolution, in modal proportions of up to 2%. The individuals have a black to golden color, ellipsoidal morphology with rounded edges, and approximately 1.25 cm in diameter by 3.0 cm in length. The fossils are preserved as internal molds, intensely pyritized, with conservation of three-dimensional morphology. The second group is chaotically arranged in the strata (fig. 4.2), representing up to 1.5% of the individuals, with a taphonomic signature characterized by a low degree of abrasion and corrosion, partial fragmentation and low dissolution. The specimens have a black to golden color, ellipsoidal morphology and approximately 2.0 cm in diameter by 3.25 cm in length. The fossils are preserved as an external mold and intensely pyritized.

4.3.2.1.2 Bivalves

Bivalve specimens have different distributions and are subdivided into two groups. A group arranged in the strata (fig. 4.3), with taphonomic signature characterized by a medium degree of abrasion and corrosion, intense fragmentation and low dissolution. This group is present in modal proportions of up to 1.8%. The individuals have a gray to golden color, with a rounded morphology. The dimensions vary from approximately 1.0 cm in the largest diameter to 2.2 cm in the smallest diameter. The fossils are preserved as an external mold, partially pyritized. The second group shows individuals arranged in a chaotic manner, usually perpendicular to the bedding plane (fig. 4.4), with a taphonomic signature characterized by a reduced degree of abrasion and corrosion, partial fragmentation and low dissolution, representing up to 1.5% of the rocks analyzed. The individuals in the second group exhibit black to golden color, arched cylindrical morphology with closed internal structure, and

approximately 2.5 cm in diameter. The fossils are preserved as an internal mold, whose three-dimensional morphology is replicated due to the presence of pyrite.

4.3.2.1.3 Bryozoan

The specimens of bryozoans are arranged in the strata, with a taphonomic signature characterized by a low degree of abrasion and corrosion, partial fragmentation, low dissolution and well preserved, present in up to 1.2% of the analyzed samples. The individuals present golden to whitish coloration, with box-like arrangement and hemispheroidal morphology, exhibiting dimensions of 1.6 cm of the largest diameter by 1.2 cm of the smallest diameter (fig. 4.5). The bryozoans occur predominantly in oblique sections and present sub-rectangular and equidimensional zoécios, commonly smaller than 1 mm. Subangular specimens occur locally, exhibiting 1.6 cm long by 1.5 cm wide (fig. 4.6). The bryozoans are preserved as an external mold and partially pyritized.

4.3.2.1.4 Thalassinoides Ichnofossils

The fossil features of Thalassinoides are chaotically arranged in the strata (fig. 3), with a taphonomic signature characterized by a high degree of abrasion and corrosion, partial fragmentation and low dissolution. These specimens are present in up to 15% of the modal proportion. The individuals present tubular excavations with preserved branching as horizontal endostratic traces allocated in the massive clay and embedded in fossil trunks (fig. 3.3). The fossiliferous filling of the tubes is composed predominantly of gastropods, bivalves and bryozoans (fig. 3.4). The tubes have variable dimensions with approximately 1.5 to 6 cm in diameter and oval cross-section. They do not have intersections, but several Y-branches that form a complex pattern of connections (Fig. 3.1 and 3.2). Filling fossils are preserved as an external mold, partially pyritized (Fig. 3.4).



Figure 3 - Taphonomic configuration of the thalassinoid traces: 1 and 2) Tubular morphology with “Y” branch preserved as horizontal endostratic traces allocated in the massive claystone forming a connection network connected to the matrix / sediment and the plant portion; 3) Vegetable filling in the inner portion of the thalassinoids occurring as encrusted with fossil trunks; 4) Internal filling of thalassinoids are composed predominantly of gastropods (E), external molds (A) of internal bivalves (B, C) and bryozoans (D), spine of equinoids (F) ?. (Scale 1, 2 and 3 - 5 cm; 4 - 2 cm).

4.3.2.2 Flora

4.3.2.2.1 Trunks

The incarbonized trunk fossils exhibit black color and are arranged parallel to the bedding plane, presenting different characteristics. Well-preserved trunks (stems), 10-12 m long and 75.0-80.0 cm in diameter. They are characterized by a low degree of abrasion and corrosion, reduced fragmentation, low dissolution and conservation of three-dimensional morphology. Longitudinally, the specimen's contour is tabular to cylindrical and its internal structure is marked by straight and parallel grooves, dense and evenly spaced (fig. 4.8). Otherwise, in a cross section (fig. 4.10), there is a whitish-gray color. It is covered by a layer of ferruginized sediments and internally marked by traces of pyritized Thalassinoides (fig. 3). Pyrite also occurs in a widespread manner along the fossil trunks and in the adjacent matrix.

Trunk fragments 0.5 mm to 4 cm long show a medium degree of abrasion and corrosion, partial fragmentation and low dissolution. Longitudinally, deformations occur due to mechanical compaction and highlighted by the crystallization of pyrite, replacing partially (fig. 4.9; 4.10) or totally (fig. 4.7) the wood fragments. The trunk fragments have a black to golden color, tabular morphology, and varying dimensions from 0.2 mm to 2 cm in diameter.

4.3.2.2.2 Leaves

The fossil leaves are arranged parallel to the bedding plans, partial to fully preserved as incarbonized impressions in the clay layers. The leaves have lenticular to subangular morphology, and black color with golden portions due to the spread of pyrite (fig. 2). Whole leaves are 4-6 cm long by 2-4 cm wide. The taphonomic signature of these fossils is characterized by a low degree of abrasion, reduced fragmentation and low dissolution.

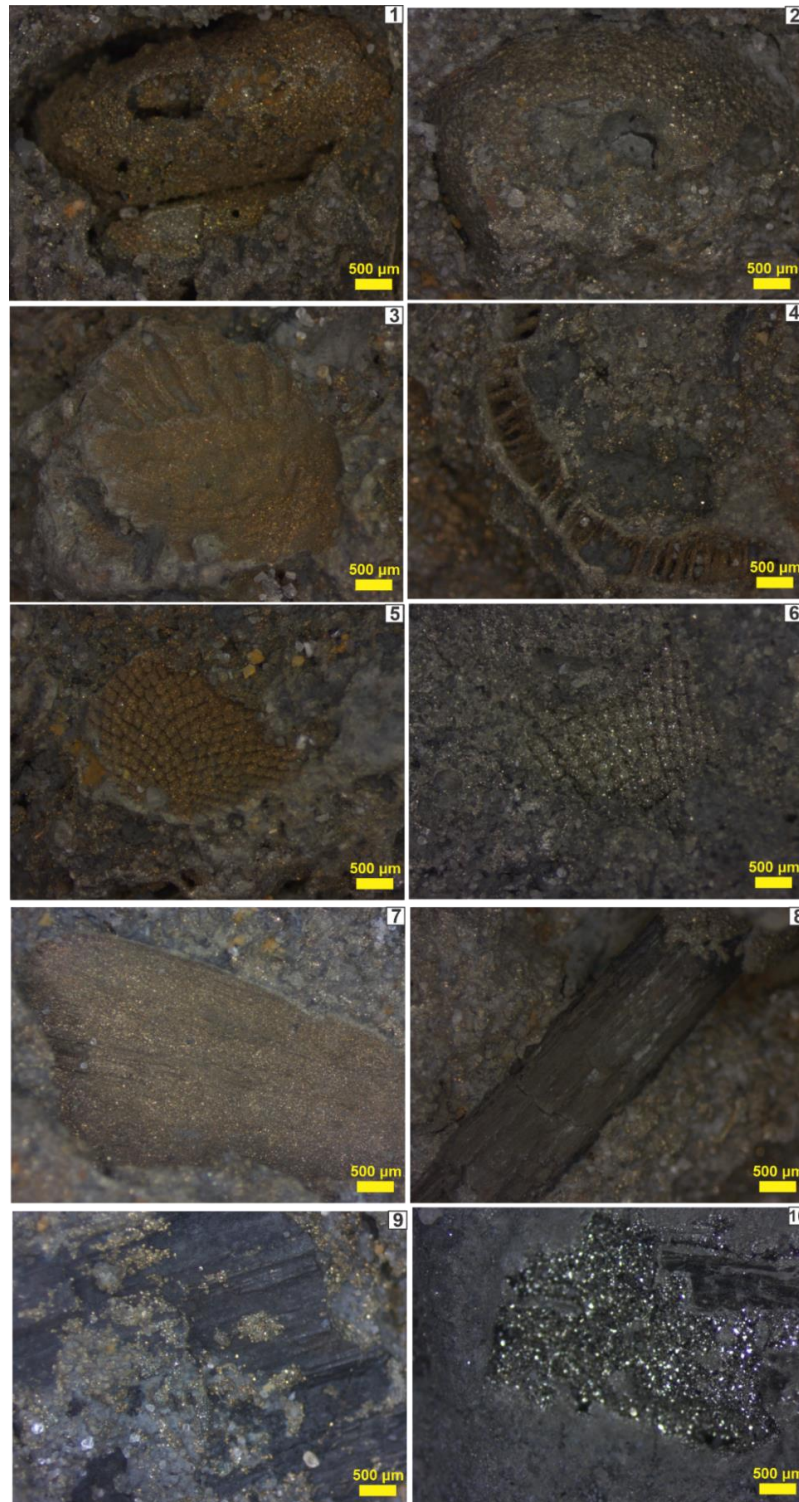


Figure 4 - Macroscopic Description: 1) Specimen of gastropods arranged in an oriented manner, with a high degree of abrasion and corrosion, intense fragmentation, low dissolution and partial preservation; 2) Specimen of gastropod arranged in a chaotic manner, reduced degree of abrasion and corrosion, partial fragmentation, low dissolution and partial preservation; 3) Bivalve specimen disposed in an oriented manner in the strata with medium degree of abrasion and corrosion, intense fragmentation, low dissolution and partial preservation; 4) Bivalve specimen arranged in a chaotic manner, allocated perpendicular to the bedding plan, reduced degree of abrasion and corrosion, partial fragmentation, low dissolution and partial preservation; 5 and 6) Specimens of bryozoans arranged in an oriented manner, low degree of abrasion and corrosion, partial fragmentation, low dissolution and high preservation; 7) Fragment of trunk totally pyritized; 8) Trunk fragment without apparent crystallization; 9 and 10) Partly pyritized trunk fractions.

4.4 PETROGRAPHY AND GEOCHEMISTRY

4.4.1 Petrography setting

The rock matrix is clay and greenish-gray in colour, rich in organic matter. Siliciclastic-carbonate matrix grains support the rocks, with an open to the normal framework and with bioclasts of granulometry varying from 0.5 to 4 mm. The lithotypes have very fine-to-fine granulometry, with moderately selected and subangular grains.

The diagenetic bioclasts contents in the samples were represented by almost 0.6% to 1.8% and are randomly distributed in a chaotic arrangement. These meso to macro bioclasts consist of gastropods (1.5%), bivalves (1.4%), bryozoans (1.8%). In addition bioclasts contents observed only in thin sections were represented by echinoderms (1.7%), ostracodes (1.6%), and green algae (<1%). Bioclasts are originally composed of calcite and occur entirely fragmented, floating in the clayey matrix. In addition, angular to subangular quartz grains, with abrupt extinction and weak wavy extinction, occur dispersed in the matrix and represent 23.5% of the rock. Feldspars were rare, especially alkali-feldspars (0.5%). The clayey matrix was the largest sample component (67.4%), rich in organic matter, and partially fills the inner pores of bioclasts (e.g., echinoderms, ostracodes, and bivalves). Wood fragments occur such as amorphous to irregular masses, light brown to black in color and length up to 4 mm. These wood fragments have angular and slightly serrated ends, moderate birefringence, and undulating extinction.

Calcite bioclasts of gastropods (sizes 45 - 50 μm) have an aleatoric arrangement into the clay matrix and the filled contents were partially replaced with pyrite (fig. 6.6). The bivalve bioclasts (sizes 150 - 200 μm) have disarticulated valves replaced by calcite, and the inner contents were filled with pyrite (fig. 5.13). The aragonite bryozoan bioclasts (sizes 0.5 - 1 mm) were replaced by calcite and then by pyrite. The calcite ostracod bioclasts (sizes 20 - 100 μm) were mostly disarticulated and were partially or totally replaced by pyrite (fig. 5.14). The calcite echinoderm bioclasts (sizes 100 - 200 μm ; fig 5.4) were partially or totally replaced by pyrite (fig. 5.1; 9.9; 5.10).

Calcite foraminifer bioclasts could be divided by sizes in the largest specimens (sizes 100 - 120 μm ; fig. 5.6) and smaller specimens (sizes \sim 20 μm ; fig. 5.13). The largest foraminifer has a partial replacement by pyrite and the smaller foraminifera were totally replaced. The calcitic envelope of green algae bioclasts (sizes \sim 4 mm) was filling with pyrite (fig. 5.3). Other undifferentiated fossil bioclast fragments (sizes 50-150 μm) amorphous-shape or circular-shape has shown ferruginized edges (fig. 5.12; 5.2; 5.3; 5.4; 5.5). Spines of echinoderms (fig. 6.1) occur locally, showing dimensions around 100 μm and partial filling by pyrite.

4.4.2 Depositional constituents

Calcite or aragonite invertebrate fossils were partial to completely replaced by pyrite, preserving the original morphology. Pyritization occurs mostly in the outer surface of gastropods and echinoderms, while replacing bivalves, bryozoans, ostracodes, and green algae externally and internally, and also in the filled molds. Pyrite is also widespread over the flora and in the clayey matrix.

Calcite cement exhibits heterogeneous distribution, mainly as a filling of secondary pores, although it also rarely fills primary pores. This cement is distributed in a heterogeneous way, commonly associated with bioclasts. The pores can be primary, according to the bioclast morphology, or secondary pores, including elongated pores, vugs, and shelter-shape, the latter related to bivalves. The primary pores are filled with clay material and rich in organic matter from the matrix, while the secondary pores were mainly filled with calcite cement.

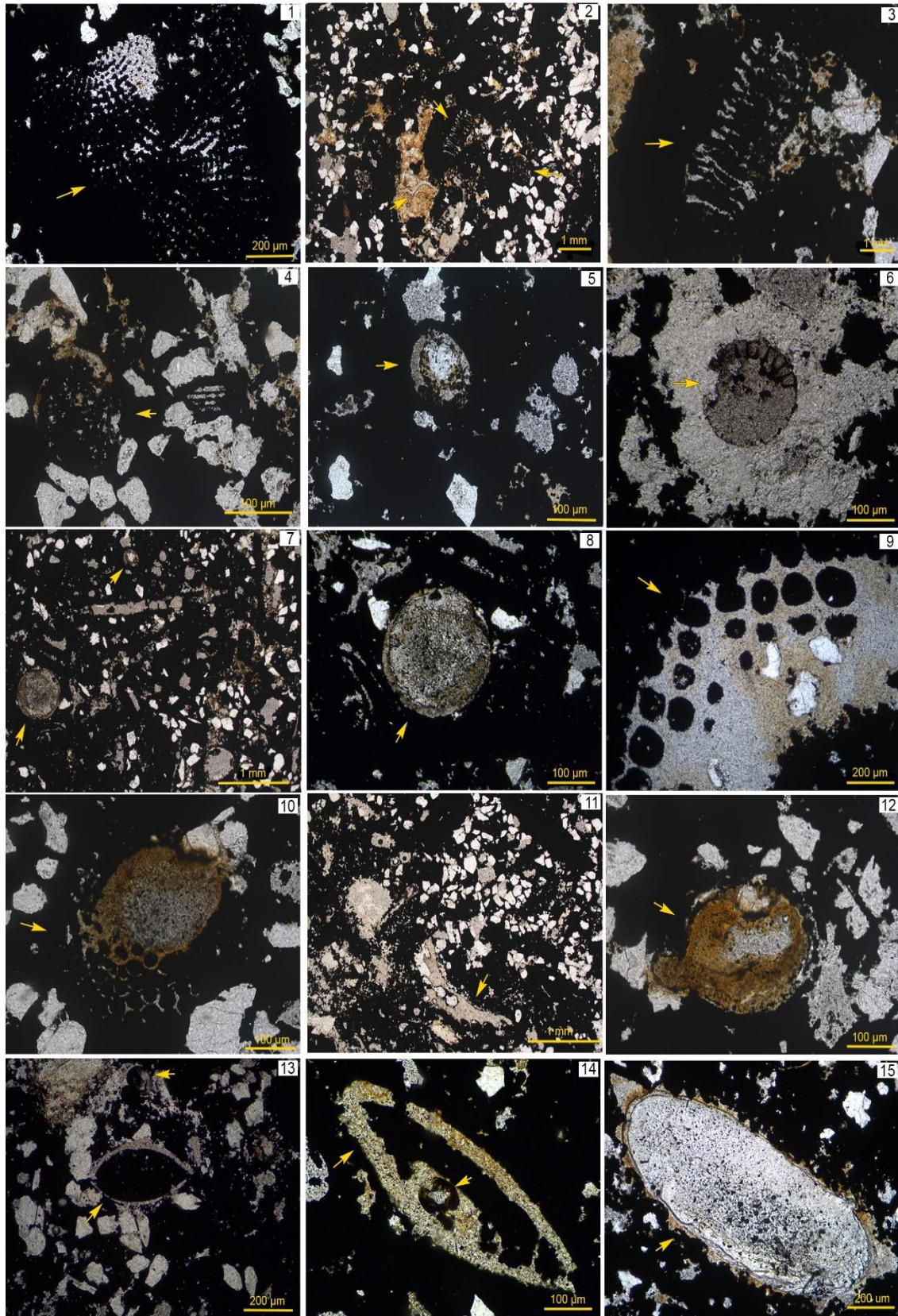


Figure 5 - Petrographic Description of the Fossils. 1) echinoderm; 2) Bryozoa; 3) Green algae; 4) Ostracodes; 5) Ostracode; 6) Foraminifero; 7) Ostracode; 8) Ostracode; 9) Echinoderm; 10) Echinoderm; 11) Bryozoa; 12) Ind.?; 13) Bivalve and Foraminiferous; 14) Ostracode; 15) Ind.?.

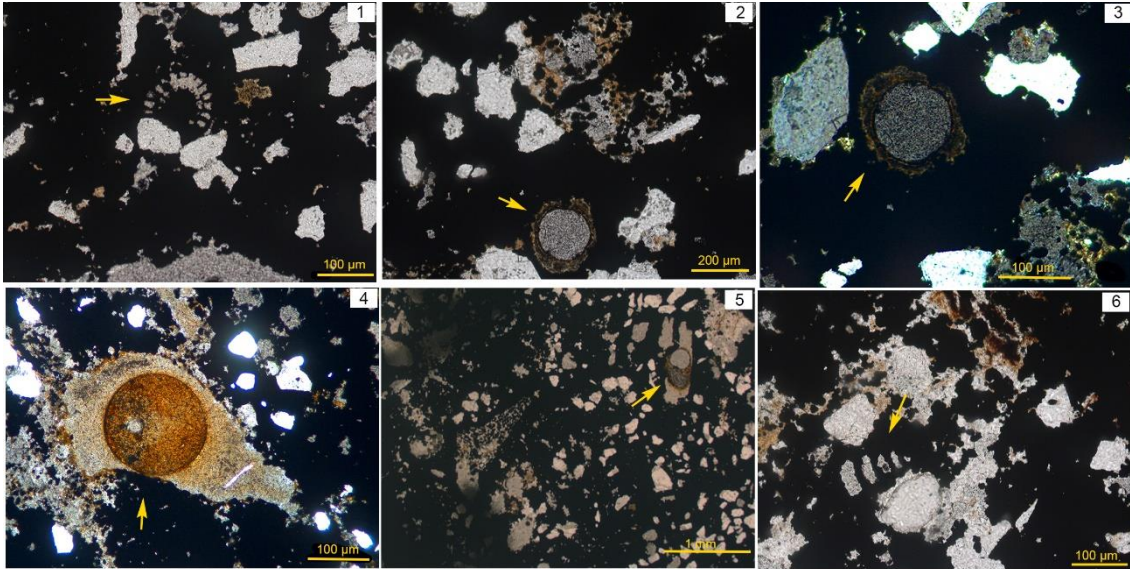


Figure 6 - Petrographic Description of Fossils. 1) Spine of echinoderm; 2) Ind.?; 3) Ind.?; 4) Ind.?; 5) Ind.?; 6) Gastropod.

4.4.3 Crystallography setting

The pyritized samples of trunks and wood fragments has two different morphotypes of crystal patterns: 1) amorphous pyrite crystals at the wood surfaces showing serrated-shape edges or fringe-shape with crystal size between 4 and 20 μm (fig. 7.4, arrow 1; and, 7.5, arrow 2) cubic pyrite crystals exclusively in the filling zone of wood with crystal sizes around 30 μm (fig. 7.6. arrow 2) and with associated amorphous crystals largest that 100 μm (fig. 7.6, seta 1). Leaves crystal were taped-shape and needle-shaped range in size between 5 to 50 μm , helically arranged, dispersed form over an amorphous matrix, with no signs of apparent pyritization (fig. 7.7, arrow 1 e 7.8, arrow 1). The recording of this morfo-textural pattern was also observed close to the areas of identification of wood fragments (fig. 7.8, arrow 2).

The specimens of bivalves from the pyritized zone have framboids and euhedral crystals (octahedral and cubic) that range in size between 5 to 10 μm (fig. 7.1, arrow 1) and anhedral to subhedral crystals that range in size between 10 to 15 μm (fig. 7.2, arrow 2). The octahedral crystals are idiomorphic without inner structure, making locally the surfaces of pyrite framboids. Pyrite crystal from gastropod molds was octahedral and cubic crystals shape that range in size between 5 to 20 μm (fig. 7.2, arrow 1), with apparent overgrowth of amorphous silica crystals (fig. 7.2, arrow 2). Bryozoan molds have euhedral (octahedral) crystals, ranging from 4-10 μm (fig. 7.3, arrow 1), as well as overgrowth of apparent amorphous silica crystals (fig. 7.3, arrow 2).

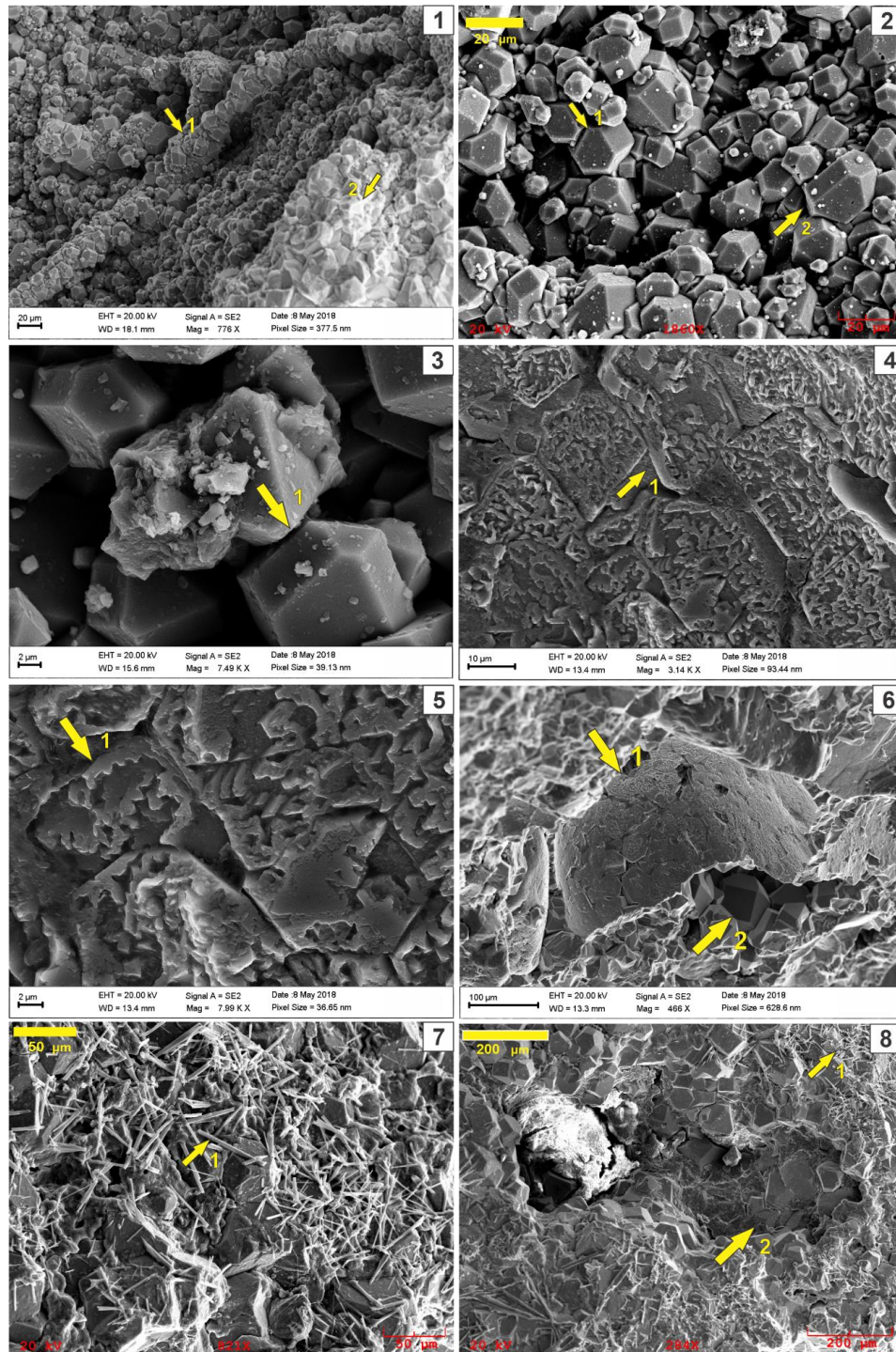


Figure 7 - Crystallographic description of pyrite crystals from SEM analysis. 1) Framboidal pyrite in bivalves, occurring as a filament of euhedral crystals (octahedral and cubic), with size between 5-10 μm (arrow 1), and aggregate of anhedral to subhedral crystals, size between 10-15 μm (arrow 2); 2) Euhedral pyrite in gastropods, occurring as octahedral and cubic crystals, well developed, with variable size between 5-20 μm (arrow 1) and overgrowth of amorphous silica crystals (arrow 2); 3) Euhedral pyrite in bryozoans, well-developed crystals, whose size varies between 4-10 μm (arrow 1), as well as overgrowth of apparent amorphous silica crystals (arrow 2); 4) Amorphous Framboidal Pyrite in wood / trunk fragments, variable in size between 4-20 μm (arrow 1); 5) Amorphous Framboidal Pyrite in fragments of wood / trunk with serrated edges or in the form of a "fringe" (arrow); 6) zone filled by pyrite crystals in wood fragments, with cubic shape, and apparent size of 30 μm (arrow 2), amorphous pyrite crystals associated with wood, size 100 μm (arrow 1); 7) Acicular pyrite in leaf impressions, with variable size between 5-50 μm (arrow 1) helically arranged; 8) Acicular pyrite in leaf impressions observed close to the areas of identification of wood fragments (arrow 2).

4.4.4 Elemental geochemistry

The qualitative chemical composition of the material was obtained through energy dispersion x-ray spectrometry (EDS) performed in point analyzes (shots) under crystallographic regions with distinct morpho-textural patterns in gastropods (fig. 8), logs (fig. 9) and trunk fragments (fig. 10), and leaves (fig. 11). In gastropods, whose morpho-textural pattern is very similar to that observed in bivalves and bryozoans (fig.8.2), two shots were taken in cubic and octahedral pyrite crystals, so that both shots clearly identified the presence of Fe and S as the main elements, in addition to carbon C and O in smaller quantities (fig. 8.1). In the analysis carried out on the trunk, using amorphous pyrite as a morpho-textural pattern as specific crystallography (fig. 9.1), two shots were taken, so that both presented an equivalent response, identifying peaks Fe, S, C and O, in addition to identifying the presence of Al in a smaller amount.

In the analysis carried out on wood fragments (fig. 10.1), which made up the matrix, 4 shots were made with three different chemical signatures: the first shot made on the fragment with amorphous textural pattern, indicated the predominant presence of Fe, S, S and O, and, to a lesser extent, aluminum Al; the third shot made on the matrix, in addition to the Fe and sulfur S peaks, identified the presence of C and O; the fourth shot made on a fragment filling zone formed by well-developed octahedral pyrite crystals, presented Fe and S as the main elements. In the analysis performed on leaf impressions (fig. 11.1), 3 shots were made: the first, reaching the texture / needle shape, showed peaks of C, O and S and in a smaller amount, signs of K, Na, Fe and Al; the second and third shots, carried out on an apparent matrix, indicated, in addition to the elements of the leaves, the presence of Fe, Si and magnesium Mg.

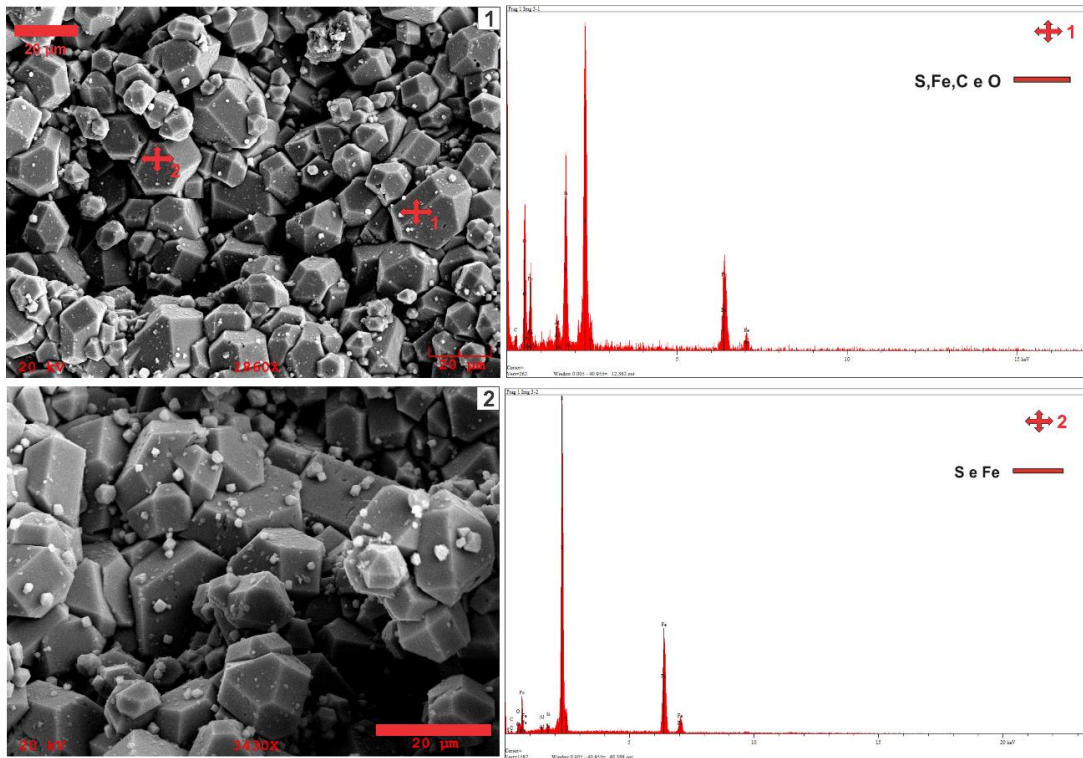


Figure 8 - Chemical analysis by EDS. 1 and 2) SEM image of a sample of inverters of gastropods, bivalves and bryozoans showing cubic and orthopedic pyrite crystal with x-ray diffraction crystallogram showing the 2θ peaks of S, Fe, C and O in shot1 and ray diffraction -x showing the 2θ peaks of S, Fe, C and O in shot2.

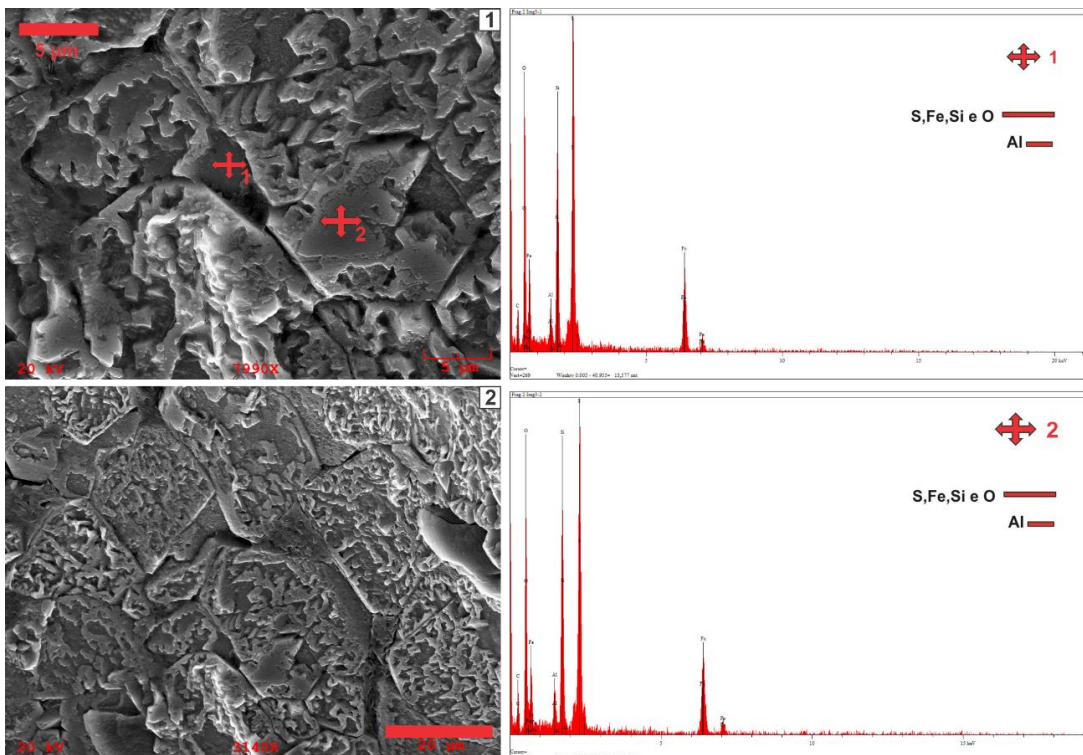


Figure 9 - Chemical analysis by EDS. 1 and 2) SEM image of a trunk sample showing an amorphous pyrite crystal framboid with x-ray diffraction crystallogram showing the 2θ peaks of S, Fe, Si and O, in addition to Al in shot1 and shot2.

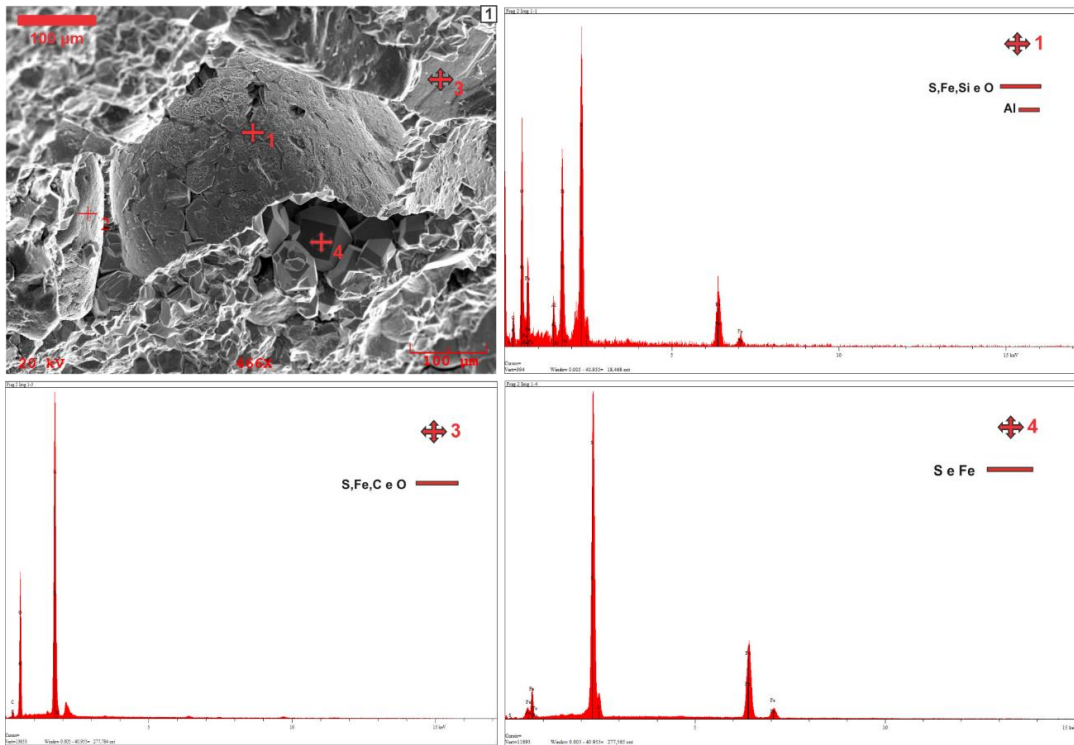


Figure 10 - Chemical analysis by EDS. 1) SEM image of a trunk sample showing a framboid in amorphous pyrite crystal, with octahedral pyrite filling zones with x-ray diffraction crystallogram showing the 2θ peaks of S, Fe, Si and O, in addition to Al in shot , presence of C in shot3 and high concentrations of S and Fe in Shot4.

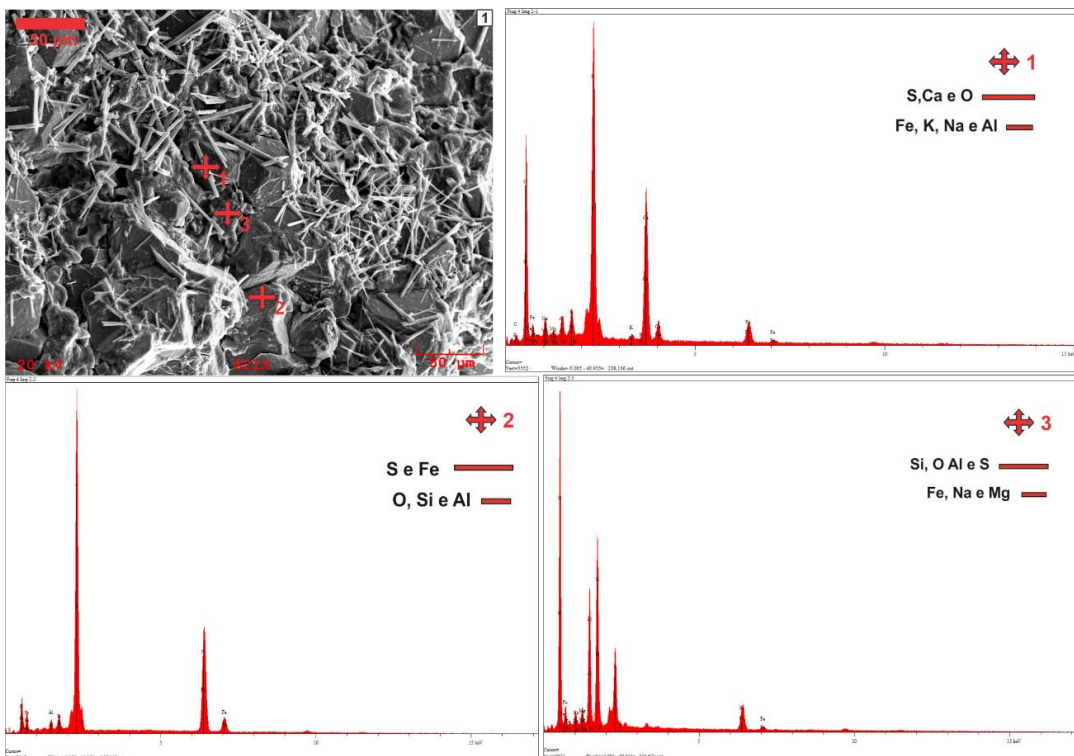


Figure 11 - Chemical analysis by EDS. 1) SEM image of leaf sample showing pyrite acicular crystals with x-ray diffraction crystallogram showing the 2θ peaks of S, Ca, O, Fe, K, Na, and Al in shot1; X-ray diffraction crystallogram showing the 2θ peaks of Si, O, Al, S, Fe, Na and Mg in shot2; X-ray diffraction crystallogram showing the 2θ choices of S, Fe, O, Si and Al in shot3.

4.4.5 X-ray diffractometry (DRX)

From X-ray diffractometry performed on the sandy-clay matrix that houses the invertebrate fossils, the mineralogical assemblies of the profiles of the zones described above were identified, essentially composed of the minerals: Pyrite (Py), Quartz (Qtz) (fig. 12), in addition to Marcasite and Spinel (fig. 13). Marcasite is a natural polymorph of pyrite that occurs as an indication of the substitution of one mineral phase by the other, while spinel is an oxide that was generated by the association of the minerals observed in the microscopy (Mg, Al and O) from the reaction of the carbonate material with the aluminum present in the system.

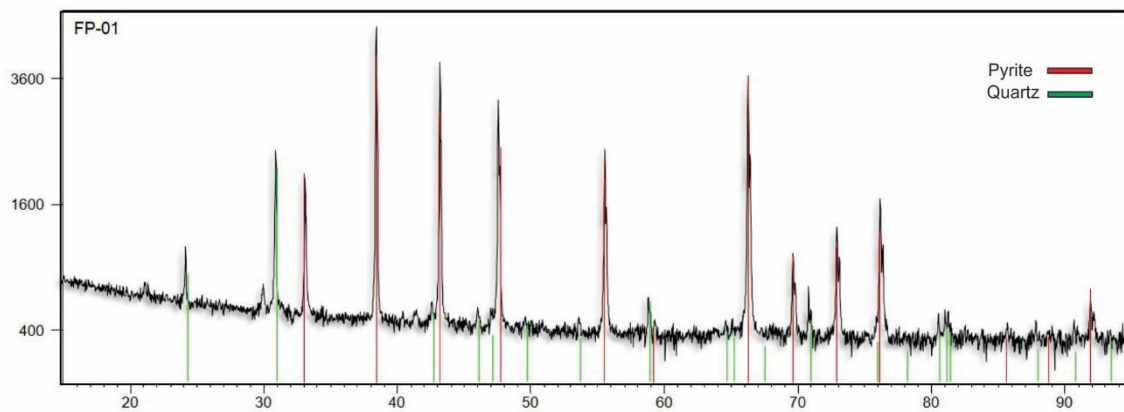


Figure 12 - X-ray energy dispersion spectrum of invertebrate individuals. The main mineralization (Py and Qtz), corroborates what was highlighted in the analysis by EDS, defining that silicification represents the initial change associated with sulfide.

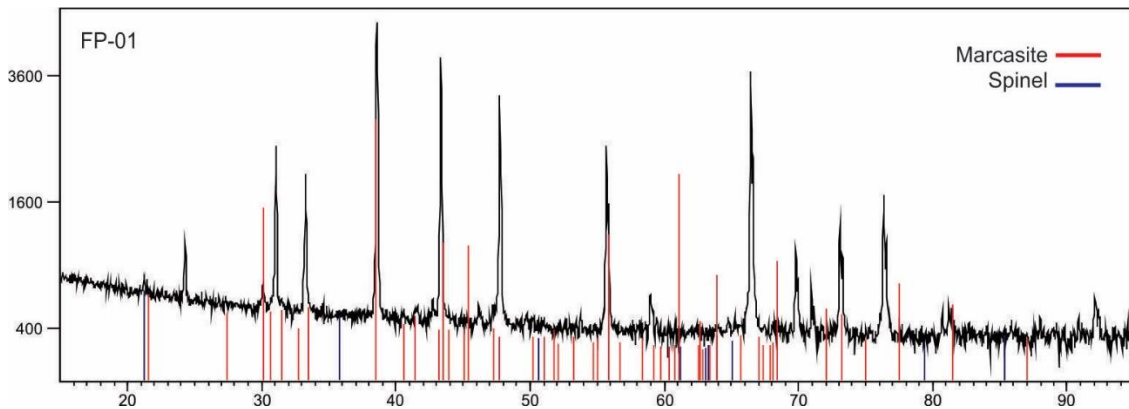


Figure 13 - X-ray energy dispersion spectrum of invertebrate individuals. In addition to the main mineralization, Marcassita, a polymorph of Pyrite, stands out, highlighting the increase in the pH of the environment or the increase in the temperature of the system.

4.5 DISCUSSION

The Pirabas Formation emerges on cliffs in the coastal zone of the states of Maranhão, Piauí and Pará, characterized by carbonate rocks and clay from Oligo-Miocene age (Maury 1925, Petri 1957, Ferreira 1966, 1982, Fernandes 1984), covered by siliciclastic miocene

deposits of the Barreiras Formation (Rosseti 2001), both overlapping, discordantly, by the Post-Barreiras sediments (Góes *et al.* 1990). The paleontological works considered historical references for the description of the fauna and flora of this unit are those of White (1887) and Maury (1925) for mollusks, bryozoans and corals; Petri (1957) contributions to foraminifera, Beurlen (1958) to crustaceans, Santos (1958, 1967) to equinoids, Santos and Travassos (1960) to fish, Paula-Couto (1967) to sirenids and Duarte (2004) in paleoflora. More recent references on records of different fossil taxa are in Távora *et al.* (2007), Aguilera & Paes (2012), Aguilera *et al.* (2013, 2017a, b), bryozoan taxonomy (Ramalho *et al.* 2015, 2017, Muricy *et al.* 2016) and the ostracod taxonomy and biostratigraphy (Nogueira and Nogueira 2017).

Berner (1970), with regard to paleontological aspects, states that the presence of pyrite produced by the reaction of hydrogen sulfite in bacteria with minerals containing iron found in marine sediments suggests that over the years, the amount of this mineral has varied and, through its oxidation, has contributed to a variation in the pH of the water in which the material was deposited. For Gu *et al.* (2020) pyrite is extremely reactive, abundant in the earth's crust, its oxidation is an important regulator in biogeochemical, weathering and oxidative processes, being related to the formation of the four most common elements on Earth: sulfur, oxygen, carbon and iron. According to Renac *et al.* (2020), metal uptake by autogenous carbonates and pyrite is related to conditions of fresh water (composition, Eh-pH), dissolved detrital particles and crystallization processes, with absorption/desorption of metals and metalloids. Crystallization of autigenic carbonate and pyrite in water is the consequence of processes such as changes from oxide to anoxic conditions, and transitions from biotic to abiotic environments (Rickard 2007).

In mangrove environments, the metal accumulation processes can be very intense and because it is a highly reducing environment, the accumulation is initially controlled by the formation of insoluble sulfides. The metals associated with the oxides-hydroxides of Fe and Mn and part of those associated with organo-metallic complexes are released when they reach the transition zone between the oxic and anoxic horizons and can migrate to the permanently anoxic levels, through the sulfide-rich interstitial waters, precipitating in the form of insoluble sulfides (Förstner & Wittman 1981, Salomons & Förstner 1980).

The details of the fossiliferous assemblies identified demonstrate that the relationships between the sub-environments of the Pirabas Formation present greater variation and complexity than originally proposed, indicating a taphonomic response originating from continental processes, characterized by low oxygen content (anoxic environment) and high

energy level. The high degree of pyritization observed in gastropods (fig. 4.1; 2), bivalves (fig. 4.3; 4) and bryozoans (fig. 4.5; 6), in these sub-environments, are usually associated with deposits that indicate anoxic conditions, associated with low oxygen circulation, promoting greater concentration and maturation of organic matter. The presence of fossil fragments as well as the different orientations in the lodging plan, suggest deposition in a high energy environment, with the action of tidal currents and waves, and possibly a storm, responsible for the reworking of the substrate.

In the Thalassinoids (fig. 3), the pyritized portion occurs filling the entire modal space (internal and external portion), including even the individuals present (mainly bivalves), the occurrence of fossil Thalassinoides traces suggest salinity fluctuations in the depositional environment (Guimarães Netto & Rossetti 2003, Guimarães Netto *et al.* 2007), *Sinusichnus* are common in environments rich in organic matter and low energy, with an abundant accumulation of carbonate mud (Gibert *et al.* 1999).

The mineralogy highlighted in the present work indicates that a large part of the wood fragments demonstrates selective pyritization so that the pyrite does not replace the original cellular material, but precipitates inside the original voids or in the voids left after the cellulose decomposition (fig. 4.9) which is less resistant to bacterial decomposition (Grimes *et al.* 2001). The most resistant portion (Grimes *et al.* 2001, Brock *et al.* 2006) is not pyritized due to the greater resistance of lignin (fig. 4.8). Given the anoxic conditions, rarely entire wood fragments are completely pyritized (fig. 4.10) (Płachno *et al.* 2018). The leaves have lenticular to subangular morphology, presenting rare incarbonized records in the greenish solid claystone (Fig. 2). The formation of pyrite during the decomposition of organic tissues from recent plants has been documented in laboratory experiments (Grimes *et al.* 2001, Brock *et al.* 2006), so it occurs when the debris reaches the sulfate-reducing geochemical zone, where conditions Eh and pH are favorable for pyrite precipitation. Pyrite (FeS_2) is formed by the oxidation of hydrogen sulfide (H_2S) from amorphous iron monosulfide (FeS) (Schoonen 2004), thus, pyrite generally precipitates near the sulfate-sulfide stability zone, where supersaturation occurs in pore water in relation to pyrite. Depending on Eh conditions in the microenvironments of the sulfate reduction zone, pyrite precipitates in different textures (Grimes *et al.* 2001). Under the highest Eh conditions, we have the generations of the first framboidal pyrite crystals, followed by the precipitation of octahedral pyrite as a response to the reduction of the Eh value during the decomposition of organic matter.

According to Butler and Rickard (2000) the formation of autigenic minerals requires nucleation and, later, crystal growth, where nucleation is a probabilistic process and requires the juxtaposition of constituents of Fe and S in the correct orientation, so that the greater the concentration of these constituents, it is more likely that many nuclei are formed, resulting in a framboidal formation, on the other hand, if the growth rates of the crystals are controlled by the transport (diffusion) of constituents to the growing faces of already formed nuclei, they are generated ideal conditions for diffusion and, therefore, for growth, and not for nucleation generating euhedral pyrite crystals (octahedral, cubic and phyto).

The occurrence of different forms of pyrite observed in the invertebrate constituents (fig. 7.1; 2; 3), fragments of wood from the host sediment (fig. 7.4; 5), acicular crystals in the plant (fig. 7.7) and the presence of silica, reflect the different redox conditions during crystal formation. In the studied material, the amorphous pyrite framboides of the wood fragments as well as the euhedral pyrites of gastropods, bryozoans and bivalves, mainly, were located close to the water / sediment interface, so that the morphology of the raspberries and the occurrence of siliciclastic overgrowths indicate that most of them are of diagenetic origin (Bak & Sawłowicz 2000, Dustira *et al.* 2013).

The occurrence of idiomorphic crystals of octahedral pyrite in the protection zones of the wood fragments (fig. 7.6) indicates the presence of more reducing conditions than in the sediment / water interface. The anaerobic bacterial activity started immediately in the surviving organic matter of the wood (mainly cellulose) where the bacteria produced hydrogen sulfide and the lower Eh, the availability of hydrogen sulfide (from the anaerobic degradation of organic matter) enabled the precipitation of the octahedral pyrite. The preservation of the acyclic morphology present in plants is an effect of its taphonomic characteristic (Grimes *et al.* 2001).

The identified geochemistry of the material evaluated by EDS in the samples containing the invertebrate fossils (fig. 8), wood fragments (fig. 9; 10) and plants (Fig. 11). In invertebrate fossils of gastropods, bivalves and bryozoans, the predominance of Fe and S is given by the nature of precipitation in anoxic zones, in addition to these pyrite-forming elements, it is possible to observe the presence of C and O in smaller quantities, understood as a physical variation geochemistry of the environment, so that the O rates in carbonate minerals vary mainly depending on the temperature, isotopic composition and salinity of the fluids from which they precipitated, where the decrease in the temperature of the fluids causes an increase

in the O values, as well as the hypersalinity caused by evaporation, while the C values may show variations related to oxidation of organic matter.

In the chemical constituents of the wood fragments, it can be noted, in addition to presenting high Fe and S values, it also demonstrated a high pattern of silicification in the pyritized zone, highlighting the partial replacement of the original material by the sulphidized mineralized zone. The relationship of the silicified zones with large amounts of pyrite observed in the samples may suggest that silicification represents an initial change associated with sulfide. This degree of substitution shapes the contribution of iron and sulfur to carbonaceous materials within the sulfide system. In plant fossils, the presence of Al, K, Ca, Na and Mg in smaller quantities is still noticed, showing chemical diagenesis as the occurrence of an average distribution of the composition of the elements, which were present in the formation environment.

Qualitative analysis by XRD did not indicate a considerable compositional mineralogical change in the data obtained by Mev, denoting the existence of similar geochemical conditions during diagenesis. In addition to the characteristic peaks of Py and Qtz (Fig. 12), Marcasite and Spinel were identified (Fig. 13). Marcasite is a natural polymorph of pyrite that occurs as an indication of the substitution of one mineral phase by the other, while spinel is an oxide that was generated by the association of the minerals observed in the microscopy (Mg, Al and O) from the reaction of the carbonate material with the aluminum present in the system. The main mineralization determined by pyrite and quartz, corroborates what was highlighted in the analysis by EDS, defining that silicification represents the initial alteration associated with sulfide. On the other hand, the inversion of Marcasite to Pyrite is an indication resulting from the increase in the pH of the fluids due to the systemic behavior related to the reactions with the carbonate rocks or even the increase in the temperature of the system.

With regard to the paleoenvironment, recent works by Hermann & Costa (2004) on grayish claystones of the Mosqueiro Island-PA of the Barreiras Formation provide clear information about their deposition as part of a mangrove ecosystem, according to Arai (1997), who evaluated palinoflora from similar material in Ilha do Outeiro-PA, states that the deposition probably occurred during the Meso-Neomiocene, presenting data that mangrove deposits of the Barreiras Formation of Mosqueiro Island can be correlated with those of modern mangroves located in the northeastern coastal region of the state from Pará. Modern and Miocene mangroves show great similarity in their pollen signatures, which indicates a common flora and an extensive mangrove forest both in the Miocene and in the present. According to Hermann &

Costa (2004) the chemical and mineralogical environmental conditions were not the same, which can be explained by the relative nature of the contribution of detritic material (quartz), the amount of biogenic material (fragment of trunk and leaves), the amount of marine contribution and the diagenesis and autogenesis that occurred in the oldest deposits.

During the analyzes, the presence of iron sulphides in the form of individual and framboid crystals was verified, such occurrences were also observed in other mangrove environments (Aragon 1997, Tripathi *et al.* 2019) and more recent research (Schieber 2002, Araújo *et al.* 2012, Renac *et al.* 2020). The crystals of iron sulphides were identified (fig. 7) showing different morpho-textural patterns: i) euhedral (fig 7.2); ii) amorphous (fig. 7.4; 7.5); iii) aggregates forming a framboid (fig. 7.1). According to Wilkin & Barnes (1996), the sequence in the degree of aggregation of iron sulphide microcrystals is explained as being a result of four steps: 1) nucleation and growth of iron monosulfide microcrystals; 2) transformation of microcrystals into greigite (Fe_3S_4); 3) aggregation of uniformly sized greigite crystals (in the framboid growth); and, finally, the replacement of the greigite framboids by pyrite. The nucleation and growth of microcrystals, in these mangrove environments, occur through a progressive conversion of thermodynamically unstable iron monosulfides so that iron sulfide supersaturation, resulting in framboidal pyrite, is spatially associated with organic matter (Wilkin & Barnes 1996).

The interactions of clayey material with iron sulfides and framboids were also observed by Aragon (1997) and were discussed by Drobner *et al.* (1990) suggesting that clays in these environments are sulfitized by the diffusion of H_2S . In this process, the iron ion present in the clay is first converted to FeS , and later to FeS_2 . Thus there would be a direct link between clays and iron sulfides. Sawlowicz (1993) states that during the process of homogenization of the framboid, substances such as organic matter or clays, common in the interstices of the structure, can be expelled or trapped as inclusions (fig 7.6).

Finally, the importance of mangrove estuaries worldwide must be taken into account. According to Souza *et al.* (2018), it can be said that mangroves provide highly relevant services to humanity, mainly as a source of resources, however, there are more specific functions regarding their role in physical processes on the coastline and their influence on adjacent ecosystems. On the coastlines, mangroves mitigate the force of the waves with their intricate root system, providing stabilization and avoiding erosion (retrogradation). The mesh formed by the roots of the mangroves helps to compact the sediment along the shore, preventing erosion and helping to retain the supply of sediment from the continent, functions that prevent the silting

up of rivers and channels bordering this ecosystem. The soil particles reach the mangrove through high tide, being captured by the root system and deposited there during low tides. Thus, the margin of estuarine systems may indicate areas of lesser water competence, where sediment particles can be deposited forming muddy banks (areas of progradation), while in areas of greater water competence (areas of retrogradation) sediments are removed and transported. For progradation areas, where they are deposited.

It is worth mentioning that mangroves also act as biological filters, retaining particles, pollutants and impurities suspended in the water. The reduction of sulfate, by oxidation of organic matter, produces sulfides that precipitate heavy metals favoring the purification of the system water, since such pollutants are trapped in the sediment, that is, as long as the muddy substrate remains anoxic, these metals will be retained in it. For Kavanagh, (2007), the growing growth pressures in the coastal zone, combined with the loss of area due to climate change, reinforce and support the need to conserve, protect and / or recover these estuarine mangrove ecosystems worldwide.

4.6 DIAGENESIS

The occurrence of clay rich in organic matter and well-preserved fauna and flora fossils indicates a low-energy environment with high primary productivity. The degree of preservation of the fossils, sometimes with preservation of the three-dimensional morphology, and the open framework of the claystone, suggests that the main diagenetic events occurred during eodiagenesis, without the occurrence of significant mechanical compaction. Pyritization also occurred in the early stages of diagenesis and pervasively, affecting individuals of fauna and flora in different ontogenetic stages, in addition to filling in fossil traces. Invertebrate fossils and trunk fragments also underwent incarbonization processes, with pyritization covering these individuals in a widespread manner. These aspects show that anoxic and free sulfur conditions were established in the environment, defined as mangroves.

Four distinct types of pyrite have been developed according to the type of fossil on which they occur: 1) octahedral pyrite in invertebrate fossils; 2) cubic pyrite in invertebrates and fossil trunks; 3) amorphous pyrite in fossil logs; and 4) acicular pyrite in leaves. The pyrite present in invertebrate fossils, in the fragments of trunks and leaves assume, respectively, predominantly euhedral shapes (octahedral and cubic), amorphous and acicular framboidal, deposited in marine sedimentary environments. Euhedral pyrite comprises octahedral and cubic crystals of microscopic size that develop in neutral alkaline conditions formed from saturated pores of water linked to ferrous monosulfides, highlighted in the final stage of diagenesis, which,

however, have the ability to form during the initial diagenetic state when the rate of sulfate reduction is low. The raspberries observed in the trunk fragments are formed in acidic conditions through the precipitation of pyrite crystals in the initial diagenetic stage, the dimensions of the raspberries increase through the very formation of euhedral pyrite crystals.

In this context, framboidal pyrites are developed indirectly from ferrous monosulfides (amorphous FeS, pyrite), in which such conversions occur through very fast processes, which can occur by adding sulfur or by losing ferrous iron. A close relationship between the formation of pyrite and organic material was observed in the study area, as demonstrated by the presence of biogenic materials, such as macrofossils and microfossils of invertebrate fossils, and fragment of fossilized trunk and leaves, in bioturbated clays and marl. In fact, organic materials in natural sedimentary environments are essential for the crystallization of pyrite. The main source of sulfur for the development of ferrous sulphides in sedimentary environments is derived from the reduction of bacterial sulphate.

Sulphate-reducing bacteria do not precipitate sulfides directly; its role is probably limited to the production of disulfide ions. Pyritized fossils, widespread in the study area, can be interpreted as replacing organic matter with pyrite. The replacement of soft parts occurs in sediments close to the sediment-water interface during diagenesis, in which the reduction of bacterial sulfate is relatively slow and ferrous iron is dominant. In addition, anaerobic environments are the most suitable for the fossilization of fossils. Carbonate cement occurs by heterogeneously filling primary and secondary pores, probably post-dating all the diagenetic processes described above. Locally, this cement replaces previously pyritized portions.

4.7 CONCLUSIONS

The set of stratigraphic, taphonomic, petrographic, mineralogical and geochemical data characterized in the gray-green claystones together with the fauna and flora present at Ataláia beach, northeastern state of Pará, allocated in the Pirabas Formation, provide significant evidence of their deposition. as part of a mangrove ecosystem. It was highlighted that the fossiliferous set present in the study area presents diversity and is organized in a predominantly chaotic way, being composed, taphonomically, by gastropods, bivalves, bryozoans, ostracodes and echinoderms, besides fossil remains of the *Thalassinoides* genus. The current flora includes trunks oriented parallel to the host rocks, in addition to fragments of trunks and leaf impressions arranged at random. The high concentration of iron present in the unit was confirmed by evidence of fossils of calcite or aragonite invertebrates, replaced by pyrite, preserving the original morphology. Pyritization occurs mainly on the outer surface of gastropods and

echinoderms, while replacing bivalves, bryozoans, ostracodes and green algae externally and internally, and also in filled molds. Pyrite is also widespread in flora, leaves and trunks, and in the clayey matrix. The details of the fossiliferous characteristics identified demonstrate that the relations between the sub-environments of the Pirabas Formation present greater variation and complexity than originally proposed, indicating a taphonomic response originating from continental processes, characterized by low oxygen content (anoxic environment) and high energy level in the region. The high degree of pyritization of flora and fauna in these sub-environments, shows anoxic conditions, associated with low oxygen circulation, promoting greater concentration and maturation of organic matter. In this context, the occurrence of different forms of pyrite observed in the invertebrate constituents, fragments of wood from the host sediment, acicular crystals in the plant and the presence of silica, reflect the different redox conditions during the formation of the crystal. The occurrence of clay rich in organic matter and well-preserved fauna and flora fossils indicates an environment of low energy consumption and high primary productivity. The degree of preservation of the fossils, sometimes with preservation of the three-dimensional morphology, and the open structure of the clay, suggests that the main diagenetic events occurred during eodiagenesis, without the occurrence of significant mechanical compaction. Pyritization also occurred in the early stages of diagenesis and in a generalized way, affecting individuals of fauna and flora in different ontogenetic stages, in addition to filling in fossil remains. Invertebrate fossils and trunk fragments also underwent incarceration processes, with pyritization covering these individuals in general. Pyritized crystals occur with different morpho-textural patterns: euhedral, amorphous and aggregates forming a framboid. The nucleation and the growth of microcrystals in the mangrove sub-environments occur through a progressive conversion of thermodynamically unstable iron monosulfides so that the supersaturation of iron sulfide, resulting in framboidal pyrite, is spatially associated with organic matter. The interactions of the clay material with iron sulfides and raspberries were also suggesting that the clays in these environments are sulfitized by the diffusion of H_2S . In this process, the iron ion present in the clay is first converted to FeS and, later, to FeS_2 demonstrating a direct connection between the clays and the sulfides. The identified geochemistry of the material corroborated the predominance of Fe and S given by the nature of the precipitation in areas of low oxygenation and high silicification pattern in the pyritized zone, highlighting the partial replacement of the original material by the sulphide mineralized zone, so that of the silicified zones with large amounts of pyrite indicates that silicification represents an initial change associated with sulfide. This degree of substitution

shapes the contribution of iron and sulfur to carbonaceous materials within the diagenetic system. It is worth mentioning that the qualitative analysis by XRD did not indicate a considerable compositional mineralogical change in the data obtained by Mev, denoting the existence of similar geochemical conditions during diagenesis. Recent works by Hermann & Costa (2004), based on the results obtained by Arai (1997), approximate the data and results obtained on the Ilha do Mosqueiro to the Northeastern portion of the State of Pará, housing the study area, indicating or reaffirming the age by correlating the characteristics of modern mangroves with mangroves of the Neogen-myocene. These characteristics are very close to the data obtained by default in the present work, further reinforcing the search for further studies in the region as a whole.

ACKNOWLEDGEMENTS

To the Laboratory of Sedimentary Geology and to the Research Group in Sedimentary Geology, for their instrumental support, in the field and classroom work. To the Graduate Program in Geology and Geochemistry at the Federal University of Pará - PPGG UFPA. The CAPES Foundation, for the granting of the master's scholarship to the first author. COPAL/NM (Application 011/2020 p /O.A) for accepting and approving the collection of said specimens at work. To teachers, supervisors, doctors and friends, in importance Dr. Orangel Aguilera and Prof. Dr. Afonso Nogueira, who assisted in the construction of the aforementioned master's degree work.

REFERENCIAS

Aguilera O. A. & Pães E. 2012. The Pirabas Formation (Early Miocene from Brazil) and the tropical Western Central Atlantic subprovince. *Boletim do Museu Paraense Emílio Goeldi. Ciências Naturais*, Belém, **7**(1):29–45.

Aguilera O.A., Guimarães J.T.F., Moraes-Santos H. 2013. Neogene Eastern Amazon carbonate platform and the palaeoenvironmental interpretation. *Swiss Journal of Palaeontology*, **132**(2):99–118.

Aguilera O., Araújo O. M. O. de, Hendy A., Nogueira A. A., Nogueira A. C., Maurity C. W., Kutter V.T., Martins M.V.A., Coletti G., Dias B.B. Silva-Caminha S. A.F.da, Jaramillo C., Bencomo K., Lopes R. T. 2020. Paleontological framework from Pirabas Formation (North Brazil) used as potential model for equatorial carbonate platform. *Mar. Micropaleontol.* **154**: 1–23.

Aguilera O., Bencomo K., Araújo O. M. O. de, Dias B. B., Coletti G., Lima D., Silva-Caminha S.A.F.da, Polck M., Martins M.V.A., Jaramillo C., Kutter V.T., Lopes R. T. 2020. Miocene heterozoan carbonate systems from the western Atlantic equatorial margin in South America: the Pirabas formation. *Sedimentary Geology*. **407**. 105739. 10.1016/j.sedgeo.2020.105739.

Aguilera O.A., Silva G. O. A., Lopes R. T., Machado A. S., dos Santos T. M., Marques G., Bertucci T., Aguiar T., Carrillo-Biceño J., Rodriguez, F., Jaramillo, C. 2017b. Neogene Proto-Caribbean porcupinefishes (Diodontidae). *PLoS One*, **12**(7): 1-26.

Alvarez-Iglesias P., Rubio B., Millos J. 2012. Isotopic identification of natural vs. anthropogenic lead sources in marine sediments from the inner Ria de Vigo (NW Spain). *Sci Total Environ*, **437**:22–35.

Antonioli F., LoPresti V., Rovere A., Ferranti L., Anzidei M., Furlani S., Mastrouzzi G., Orru P.E., Scicchitano G., Sannino G., Spampinato C.R., Pagliarulo R., Deian G., Sabata E.de, Sansò P., Vacchi M., Vecchio A. 2015. Entalhes das marés no Mar Mediterrâneo: uma análise abrangente. *Quat.Sci.Rev.*, **119**:66–84.

Arai M. 1997. Dinoflagelados (Dinophyceae) miocênicos do Grupo Barreiras do Nordeste do estado do Pará (Brasil). *Revista Universidade de Guarulhos*, ano II (número especial): 98-106.

Aragon G.T. 1997. *Biogeoquímica sedimentar do enxofre e do ferro em um manguezal da baía de Sepetiba, RJ. neoformação de sulfetos ferrosos*. PhD Theses, Doutorado em Geoquímica Ambiental, Universidade Federal Fluminense, Niterói, 119p.

Araújo Jr. J.M. C., Otero X.L., Marques A.G.B., Nóbrega G.N., Silva J. R. F., Ferreira T. O. 2012. Selective geochemistry of iron in mangrove soils in a semiarid tropical climate effects of the burrowing activity of crabs. *Ucides cordatus* and *Uca maracoani*. *Geo-Marine Letters*, **32**:289–300.

Bak M. & Sawlowicz Z. 2000. Pyritized radiolarians from the Mid-Cretaceous deposits of the Pieniny Klippen Belt—a model of pyritization in a anoxic environment. *Geologica Carpathica*, **51**: 91–99.

Beurlen K. 1958a. Contribuição á paleontologia do estado do Pará. Crustáceos decápodes da formação Pirabas. *Boletim do Museu Paraense Emílio Goeldi*, **5**:1–49.

- Berner RA. 1970. Formação de pirita sedimentar. *Sou. J. Sci.*, **268**: 1-23
- Butler Ian & Rickard David. 2000. Framboidal pyrite formation by the oxidation of Iron (II) Monosulfide by Hydrogen Sulfide.
- Briggs D.E.G.2003. The role of decay and mineralization in the preservation of soft-bodied fossils. *Annual Review of Earth and Planetary Sciences*, **31**: 275–301.
- Brock F., Parkes J., Briggs D.E.G. 2006. Experimental pyrite formation associated with decay of plant material. *Palaios*, **21**: 499-506.
- Behling H. & Costa M.L. 2004. Mineralogia, geoquímica e palinologia de depósitos de manguezais moderno e do Terciário tardio na Formação Barreiras, Ilha do Mosqueiro, nordeste do estado do Pará, Leste da Amazônia. *J.S.Am Earth Sci.*, **17**: 285–295
- Duarte L. 2004. Paleoflórula. In: Rossetti D.F. & Góes A.M. (eds.) *O Neógeno da Amazônia Oriental*. Belém, Museu Paraense Emílio Goeldi, p. 169-196. (Coleção Friederich Katzer).
- Dustira A.M., Wignall P.B., Joachimski M., Blomeier D., Hartkopt Froder, C., Bond D.P.G. 2013. Gradual onset of anoxia across the Permian Triassic boundary in Svalbard, Norway. *Palaeogeography, Palaeoclimatology, Palaeoecology*, **374**: 303–313.
- Drobner E., Huber H., Wachtermauser G., Rose D., Stetter K. O. 1990. Pyrite formation linked with hydrogen evolution under anaerobic conditions. *Nature*, **346**: 742-744.
- Egger D. A., Bera A., Cahen D., Hodes G., Kirchartz T., Kronik L., Lovrincic R., Rappe A. M., Reichman D. R., Yaffe O. 2018. What remains unexplained about the Properties of Halide Perovskites? *Adv. Mater.*, **30**: 1800691.
- Ferreira C.S. 1966. Características lito-paleontológicas na Formação Pirabas, estado do Pará. In: 6ª Conferência Geológica das Guianas, Belém. *Anais[...]*, p.101-111.
- Ferreira C.S.M., Vicalvi A., Macedo A.C.M. 1981. Nota sobre a sequência sedimentar ao sul do rio Guamá, Estado do Pará. Evidências do Oligo-Mioceno marinho, através dos resultados preliminares da sondagem feita em Vila Mãe do Rio, (“48”), BR-010, Município de Irituia. *Anais da Academia Brasileira de Ciências*, **53**:208-209.
- Fernandes J.M.G. 1984. Paleoecology of Formation Pirabas, Pará State. In: 33º Brazilian Congress of Geology. *Anais da Academia Brasileira de Ciências*, **1**:330–340.
- Figueiredo J., Hoorn C., Van der Ven P., Soares E. 2009. Late Miocene on set of the Amazon River and the Amazon deep-sea fan: evidence from the Foz do Amazonas Basin. *Geology*, **37**: 619–622.
- Forstner U. & Wittmann G.T.W. 1981. *Metal pollution in the aquatic environment*. 2 ed. Berlin, Springer-Verlag, 486p.
- Galehouse J.S. 1971. Point counting. In: Carver R. E. (ed.). *Procedures in sedimentary petrology*. New York, Wiley-Interscience, p. 385-407.

- Góes A.M., Rossetti D.F., Nogueira A.C.R., Toledo P.M. 1990. Modelo deposicional preliminar da Formação Pirabas no Nordeste do Estado do Pará. *Boletim do Museu Paraense Emílio Goeldi*, **2**:3-15.
- Goldner A., Herold N., Huber M. 2014. Antarctic glaciation caused ocean circulation changes at the Eocene-Oligocene transition. *Nature*, **511**(7511): 574–577.
- Gibert J.M., Jeong K., Martinell J. 1999. Ethologic and ontogenic significance of the Pliocene trace fossil *Sinusichnus sinuosus* from the northwestern Mediterranean. *Lethaia*, **32**: 31-40.
- Gu X., Heaney P., Reis F.D.A., Brantley S.L. 2020. Deep abiotic weathering of pyrite. *Science* 370, doi.org/10.1126/science.abb8092
- Guimarães Netto R. & Rossetti D.F. 2003. Ichnology and salinity fluctuations: a case study in the Early Miocene (Lower Barreiras Succession) of São Luís Basin, Maranhão, Brazil. *Revista Brasileira de Paleontologia*, **6**:5–18.
- Guimarães Netto R., Buatois L.A., Mángano M., Balistieri P. 2007. Gyrolithes as a multipurpose burrow: an ethological approach. *Revista Brasileira de Paleontologia*, **10** (3):157-168.
- Grimes S.T., Brock F., Rickard D., Davies K.L., Edwards D., Briggs D.E.G., Parkes R.J. 2001. Understanding fossilization: Experimental pyritization of plants. *Geology*, **29**: 123–126, DOI: 10.1130/0091-7613(2001)0292.0.CO;2.
- Jorgensen S. S. 1977. *Metodologia utilizada para análise química de rotina: guia analítico*. Piracicaba, Cena, 24 p.
- Jorgensen B.B., Findlay A.J. Pellerin A. 2019. The biogeochemical sulfur cycle of marine sediments. *Front. Microbiol.* **10**:849. DOI: 10.3389/fmicb.2019.00849.
- Kavanagh E. 2007. A world without mangroves? *Science*, **317**: 41-43.
- Maury C.J. 1925. *Fosseis terciários do Brasil com descrições de novas formas cretáceas*. Rio de Janeiro, Serviço Geológico Mineral Brasil, 665p. (Monografia, 4).
- Muricy G. *et al.* 2016. Hexactinellid sponges reported from shallow waters in the Oligo-Miocene Pirabas Formation (N Brazil) are in fact cheilostome bryozoans. *Journal of South American Earth Sciences*, **72**: 387–397.
- Nogueira A.A.E. & Nogueira A.C.R. 2017. Ostracods biostratigraphy of the Oligocene-Miocene carbonate platform in the Northeastern Amazonia coast and its correlation with the Caribbean region. *Journal of South American Earth Sciences*, **80**: 389–403.
- Paula-Couto C. 1967. Contribuição à paleontologia do estado de Pará. Um sirênio na Formação Pirabas. *In: 1º Simpósio sobre a Biota Amazônica, Atas[...]* p. 345–357.
- Paula Couto C. de. 1967. Contribuição à paleontologia do Estado do Pará. Um sirênio na Formação Pirabas. *In: Simpósio sobre a biota Amazônica, Atas[...]*, v. 1, Geociências, p. 345-357.

Percak-Dennett E, He S, Converse B, Konishi H, Xu H, Corcoran A, Noguera D, Chan C, Bhattacharyya A, Borch T. *et al.* 2017. Aceleração microbiana da oxidação aeróbia da pirita em pH circunneutro. *Geobiologia*, **15**: 690–703

Petri S. 1957. Foraminíferos miocênicos da Formação Pirabas. *Boletim da Faculdade de Filosofia, Ciências e Letras da Universidade de São Paulo (Geologia)*, **216** (16):1-79.

Plachno B., Jurkowska A., Pacyna G., Worobiec E., Gedl P., S`Wierczewskagladysz E. 2018. Late Turonian plant assemblage from Opole (southern Poland): new data on Late Cretaceous vegetation of the northern part of European Province in the light of palaeoenvironmental studies. *Proceedings of Geological Associations*, **129**: 159–170, <https://doi.org/10.1016/j.pgeola.2018.01.008>.

Ramalho L.V., Távora V.A., Tilbrook K.J., Zágorsek K. 2015. New species of *Hippopleurifera* (Bryozoa, Cheilostomata) from the Miocene Pirabas Formation, Pará state, Brazil. *Zootaxa*, **3999** (1): 125-134.

Ramalho L.V., Távora V.A., Zagorsek K. 2017. New records of the bryozoan *Metrarabdotos* from the Pirabas Formation (Lower Miocene), Pará State, Brazil. *Palaeontologia Electronica* 20.2(32A): 1-11.

Renac C., Barats A., Mexias A., Barrière J., Rozmaric M., Gerbe M. C. 2020. Oxic and post-oxic chemical changes related to eogenesis and mesogenesis in a Miocene paleolake. *Journal of Paleolimnology*. 64. 10.1007/s10933-020-00131-3.

Rossetti D.F., Góes A.M., Souza L.S.B. 2001. Estratigrafia da sucessão sedimentar Pós-Barreiras (Zona Bragantina, Pará) com base em radar de penetração no solo. *Revista Brasileira de Geofísica*, **19**(2):113-130.

Rossetti D.F. & Góes A.M. (ed.). 2004. *O Neógeno da Amazônia Oriental*. Belém, Museu Paraense Emílio Goeldi, p. 13-52.

Rossetti D.F., Bezerra F.H.R., Dominguez J.M.L. 2013. Late Oligocene–Miocene transgressions along the equatorial and eastern margins of Brazil. *Earth-Science Reviews*, **123**:87–112.

Rickard D. & Luther G.W. 2007. Chemistry of iron sulfides. *ChemRev.*, **107**: 514–562.

Salomons W. & Forstner U. 1980. Trace metal analysis on polluted sediments. II Evaluation of environmental impact. *Environ Technol Lett* **1**:506-517

Sawlowicz Z. 1993. Pyrite framboids and their development: a new conceptual mechanism. *Geologische Rundschau* **82**:148-156.

Sanders H.L., Mangelsdorf P.C., Hampson G.R. 1965. Salinity and faunal distribution in the Pocasset River, Massachusetts. *Limnology and Oceanography*, **10**(suppl.):R216-R229.

Santos M.E.C.M. 1958. Equinóides miocênicos da Formação Pirabas. *Boletim da Divisão de Geologia e Mineralogia*, **179**:1–24.

Santos M.E.C.M. 1967. Equinóides miocênicos da Formação Pirabas. *In: 1º Simpósio sobre a Biota Amazônica, Atas[...]*, p. 407–410.

Santos R. S. & Travassos S. 1960. Contribuição à paleontologia do Estado do Pará. Peixes fósseis da Formação Pirabas. *Divisão de Geologia e Mineralogia*, Departamento Nacional da Produção Mineral, **16**:1–35.

Schoonen MAA: Sulfur biogeochemistry past and present. Edited by: Amend JP, Edwards KJ, Lyons TW. 2004, Boulder, Colorado, 117–134. Mechanisms of sedimentary pyrite formation Geological Society of America Special Paper 379.

Schieber J. 2002a. Sedimentary pyrite: a window into the microbial Past. *Geology*, **30**: 531–534.

Scholz F. & Neumann T. 2007. Trace element diagenesis in pyrite-rich sediments of the achterwasser lagoon, SW Baltic Sea. *Marine Chemistry*, **107** (4): 516-532, ISSN 0304-4203.

Severin K.P. 2004. *Energy dispersive spectrometry of common rock forming Minerals*. Dordrecht, Holanda, Kluwer Acad.

Souza C.A., Duarte L.F.A., João M.C.A., Pinheiro M.A.A. 2018. Biodiversidade e conservação dos manguezais: importância bioecológica e econômica. *In: Pinheiro M.A.A. & Talamoni A.C.B. (org.). Educação ambiental sobre manguezais*. São Vicente, UNESP, Instituto de Biociências, Câmpus do Litoral Paulista, Cap. 1, p. 16-56.

Távora V.A., Silveira E.S.F., Milhomem Neto J.M. 2007. Mina B-17, Capanema,PA - expressivo registro de uma paleolaguna do Cenozóico Brasileiro. *In: Winge M., Schobbenhaus C., Berbert-Born M., Queiroz E.T., Campos D.A., Souza C.R.G., Fernandes A.C.S. (ed.) Sítios geológicos e paleontológicos do Brasil*. Publicado na Internet em 07/01/2007 no endereço <http://www.unb.br/ig/sigep/sitio121/sitio121.pdf>.

Tripathi O. P. *et al.* 2015. The predictability of the extratropical stratosphere on monthly time-scales and its impact on the skill of tropospheric forecasts. *Quarterly Journal of the Royal Meteorological Society*, **141**(689): 987–1003.

Tripathi S. K., Resmi S., Roychaudhuri M., Karthikeyan S.I.M., Pradkan R.K. 2019. Pyrite framboids from buried paleo estuary off Chilka Lake IJG. *Indian Journal of Geosciences*. **69**: 145-154.

Watts M.E., Ball I.R., Stewart R.S., Klein C.J., Wilson K., Steinback C., Lourival R., Kircher L, Possingham H.P. 2009. Marxan with Zones: software for optimal conservation based landand sea-use zoning. *Environ. Model. Softw.*, **24**: 1513–1521.

Wilkin, R. & Barnes H.L. 1996. Pyrite formation by reactions of iron monosulphides with dissolved inorganic and organic sulphur species. *Geochimica et Cosmochimica Acta*, **60**: 4167–4179.

White C. A. 1887. Contribuições à paleontologia do Brasil. *Archivos do Museu Nacional*, **7**:1–273.

CAPÍTULO 5

5.1 CONSIDERAÇÕES FINAIS

Os trabalhos de campo e atividades de laboratório realizadas no âmbito deste trabalho de mestrado permitiu descrever um conjunto de dados estratigráficos, tafonômicos, petrográficos, mineralógicos e geoquímicos caracterizados nas argilas verde-acinzentadas juntamente com a fauna e flora presentes na praia da Ataláia, nordeste do estado do Pará, alocada na Formação Pirabas – Plataforma Bragantina, na qual fornecem evidências significativas de sua deposição como parte de um ecossistema de mangue. A flora atual inclui troncos orientados paralelamente às rochas hospedeiras, além de fragmentos de troncos e impressões de folhas dispostas caoticamente. A alta concentração de ferro presente na unidade foi confirmada por evidências de fósseis de invertebrados de calcita ou aragonita, substituídos por pirita, preservando a morfologia original. A piritização ocorre principalmente na superfície externa de gastrópodes e equinodermos, enquanto substitui bivalves, briozoários, ostracodes e algas verdes externa e internamente, e também em moldes preenchidos. A pirita também é comum na flora, folhas e troncos e na matriz argilosa.

O alto grau de piritização da flora e da fauna nesses subambientes mostra condições anóxicas, associadas à baixa circulação de oxigênio, promovendo maior concentração e maturação da matéria orgânica. O grau de preservação dos fósseis, às vezes com preservação da morfologia tridimensional, e da estrutura aberta da argila, sugere que os principais eventos diagenéticos ocorreram durante a eodiagênese, sem a ocorrência de compactação mecânica significativa.

A piritização também ocorreu nos estágios iniciais da diagênese e de forma generalizada, afetando indivíduos da fauna e da flora em diferentes estágios ontogenéticos, além de preencher restos fósseis. Este estudo corrobora trabalhos recentes de Hermann & Costa (2004), de modo que se aproximam os dados e resultados obtidos na Ilha do Mosqueiro - Nordeste do Estado do Pará, abrigando a área de estudo, indicando ou reafirmando a idade correlacionando as características dos manguezais modernos com os manguezais do Neogeno-mioceno. Essas características estão muito próximas dos dados obtidos por default no presente trabalho, reforçando ainda mais a busca por novos estudos na região como um todo.

REFERÊNCIAS

- Aguilera O. A. & Pães E. 2012. The Pirabas Formation (Early Miocene from Brazil) and the tropical Western Central Atlantic subprovince. *Boletim do Museu Paraense Emílio Goeldi. Ciências Naturais*, **7**(1):29–45.
- Aguilera O.A., Guimarães J.T.F., Moraes-Santos H. 2013. Neogene Eastern Amazon carbonate platform and the palaeoenvironmental interpretation. *Swiss Journal of Palaeontology*, **132**(2):99–118.
- Aguilera O.A., Luz Z., Carrillo-Briceño J.D., Kocsis L., Vennemann T.W., de Toledo P.M. 2017a. Neogene sharks and rays from the Brazilian 'Blue Amazon'. *PLoS ONE* **12**(8): 1-34.
- Aguilera O., Araújo O. M. O. de, Hendy A., Nogueira A. A., Nogueira A. C., Maurity C. W., Kutter V.T., Martins M.V.A., Coletti G., Dias B.B. Silva-Caminha S. A.F.da, Jaramillo C., Bencomo K., Lopes R. T. 2020. Paleontological framework from Pirabas Formation (North Brazil) used as potential model for equatorial carbonate platform. *Mar. Micropaleontol.* **154**: 1–23.
- Aguilera O., Bencomo K., Araújo O. M. O. de, Dias B. B., Coletti G., Lima D., Silva-Caminha S.A.F.da, Polck M., Martins M.V.A., Jaramillo C., Kutter V.T., Lopes R. T. 2020. Miocene heterozoan carbonate systems from the western Atlantic equatorial margin in South America: the Pirabas formation. *Sedimentary Geology*. 407. 105739. 10.1016/j.sedgeo.2020.105739.
- Beurlen K. 1958a. Contribuição á paleontologia do estado do Pará. Crustáceos decápodes da formação Pirabas. *Boletim do Museu Paraense Emílio Goeldi*, **5**:1–49.
- Berner R.A. 1991. A model for atmospheric CO₂ over Phanerozoic time. *American Journal of Science*, **291**(4): 339–376.
- Costa J.B.S., Bemerguy R.L., Hasui Y., Borges M.S., Ferreira JR. C.R.P., Bezerra P.E.L. Costa M.L., Fernandes J.M.G. 1996. Neotectônica da região amazônica: aspectos tectônicos, geomorfológicos e deposicionais. *Geonomos*, **4**(2):23-43.
- Costa J.B.S., Hasui Y., Bemerguy R.L., Villegas J.M.C. 2002. Tectonics and paleogeography of the Marajó Basin, northern Brazil. *Anais da Academia Brasileira de Ciências*, **74** (3): 519-531.
- Duarte L. 2004. Paleoflórula. In: Rossetti D.F. & Góes A.M. (eds.) *O Neógeno da Amazônia Oriental*. Belém, Museu Paraense Emílio Goeldi, Coleção Friederich Katzer, p. 169-196.
- Dunham R. 1962. Classification of carbonate rocks according to depositional texture. In: Ham W. (ed). *Classification of carbonate rocks*. Tulsa, p. 108 – 121. (AAPG. Memoir 1).
- Embry A. & Klovan J. 1971. Late Devonian reef tracts on northeastern Banks Islands, Northwest Territories. *Canadian Petrology and Geology Bulletin*, **19** (4): 730-781.
- Ferreira C.S. 1966. Características lito-paleontológicas na Formação Pirabas, estado do Pará. In: 6ª Conferência Geológica das Guianas, Belém. *Anais[...]*, p.101-111.
- Ferreira C.S.M., Vicalvi A., Macedo A.C.M. 1981. Nota sobre a sequência sedimentar ao sul do rio Guamá, Estado do Pará. Evidências do Oligo-Mioceno marinho, através dos resultados

preliminares da sondagem feita em Vila Mãe do Rio, (“48”), BR-010, município de Irituia. *Anais da Academia Brasileira de Ciências*, **53**:208-209.

Fernandes J.M.G. 1984. Paleocology of Formation Pirabas, Pará State. In: 33° Brazilian Congress of Geology. *Anais da Academia Brasileira de Ciências*, **1**:330–340.

Fernandes J.M.G. & Távora V.A. 1990. Estudo dos foraminíferos da Formação Pirabas procedentes do furo CB-UFPa- P1 (85), Município de Capanema, Estado do Pará. In: SBG, 36° Congr. Brasileiro Geol., Natal, *Anais[...]* v.1, p. 470-475.

Góes A.M., Rossetti D.F., Nogueira A.C.R., Toledo P.M. 1990. Modelo deposicional preliminar da Formação Pirabas no Nordeste do Estado do Pará. *Boletim do Museu Paraense Emílio Goeldi*, **2**:3-15.

Klein E.S. & Moura C.A.V. 2003. Síntese Geológica e Geocronológica do Cráton São Luís e do Cinturão Gurupi na região do Rio Gurupi (NE-Pará / NW-Maranhão). *Geologia-USP*, **3**:97-112.

Leite F.P.R., Oliveira M.E.B., Arai M., Truckenbrodt W. 1997a. Palinostratigrafia da Formação Pirabas e Grupo Barreiras, Mioceno do nordeste do estado do Pará, Brasil. *Revista da Universidade de Guarulhos*, **2** (esp.): 141–147.

Leite F. P. R., Oliveira M. E. B., Oliveira P. E., Silvestre-Capelato M. S., Arai M., Truckenbrodt W. 1997b. Palinofloras miocenas da Formação Pirabas e Grupo Barreiras, na Região Bragantina, Estado do Pará, Brasil. *Revista da Universidade de Guarulhos*, **2**:128-140.

Leite F.P.R. 2004. Palinologia. In: Rossetti, D.F. & Góes, A.M. (eds.). *O Neogeno da Amazônia Oriental*. Belém, Museu Paraense Emilio Goeldi, p. 55-90.

Maury C.J. 1925. *Fosseis terciários do Brasil com descrições de novas formas cretáceas*. Rio de Janeiro, Serviço Geológico Mineral Brasil, 665p. (Monografia, 4).

Moreira M., Díaz R., Santos H., Mendoza U., Böttcher M. E., Capilla R., Machado W. 2018. Sedimentary trace element sinks in a tropical upwelling system. *Journal of Soils and Sediments*, **18**(1): 287-296.

Muricy G. *et al.* 2016. Hexactinellid sponges reported from shallow waters in the Oligo-Miocene Pirabas Formation (N Brazil) are in fact cheilostome bryozoans. *Journal of South American Earth Sciences*, **72**: 387–397.

Nogueira A.A.E. 2015. *Taxonomia, paleoecologia e bioestratigrafia (ostracoda) do Oligo-Mioceno da Formação Pirabas (Estado do Pará, Brasil)*. PhD Theses Doutorado, UFPa, Belém, 362p.

Nogueira A.A.E. & Nogueira, A.C.R. 2017. Ostracods biostratigraphy of the Oligocene-Miocene carbonate platform in the Northeastern Amazonia coast and its correlation with the Caribbean region. *Journal of South American Earth Sciences*, **80**: 389–403.

Paula-Couto C. 1967. Contribuição à paleontologia do estado de Pará. Um sirênio na Formação Pirabas. In: 1° Simpósio sobre a Biota Amazônica, *Atas[...]* p. 345–357.

- Petri S. 1957. Foraminíferos miocênicos da Formação Pirabas. *Boletim da Faculdade de Filosofia, Ciências e Letras da Universidade de São Paulo, Geologia*, **216** (16):1-79.
- Ramos M.I.F., Távora V.A., Pinheiro M.P., Baia N.B. 2004. Microfósseis. In: Rossetti F.R. & Góes A.M. (eds.). *O Neógeno Da Amazônia Oriental*, Belém, Museu Paraense Emílio Goeldi, p.93-107.
- Ramalho L.V., Távora V.A., Tilbrook K.J., Zágorsek K. 2015. New species of *Hippopleurifera* (Bryozoa, Cheilostomata) from the Miocene Pirabas Formation, Pará state, Brazil. *Zootaxa*, **3999** (1): 125-134.
- Ramalho L.V., Távora V.A., Zagorsek K. 2017. New records of the bryozoan *Metrarabdotos* from the Pirabas Formation (Lower Miocene), Pará State, Brazil. *Palaeontologia Electronica* **20.2**(32A): 1-11.
- Read J.F. 1982. Carbonate platforms of passive (extensional) continental margins: types, characteristics and evolution. *Tectonophys.* **81**:195-212.
- Rossetti D.F., Góes A.M., Souza L.S.B. 2001. Estratigrafia da sucessão sedimentar Pós-Barreiras (Zona Bragantina, Pará) com base em radar de penetração no solo. *Revista Brasileira de Geofísica*, **19**(2):113-130.
- Rossetti D.F. & Góes A.M. (ed.). 2004. *O Neógeno da Amazônia Oriental*. Belém, Museu Paraense Emílio Goeldi, p. 13-52.
- Rossetti D.F., Bezerra F.H.R., Dominguez J.M.L. 2013. Late Oligocene–Miocene transgressions along the equatorial and eastern margins of Brazil. *Earth-Science Reviews*, **123**:87–112.
- Santos M.E.C.M. 1958. Equinóides miocênicos da Formação Pirabas. *Boletim da Divisão de Geologia e Mineralogia*, **179**:1–24.
- Santos M.E.C.M. 1967. Equinóides miocênicos da Formação Pirabas. In: 1º, Simpósio sobre a Biota Amazônica, Atas[...], p. 407–410.
- Santos R. S. & Travassos S. 1960. Contribuição à paleontologia do Estado do Pará. Peixes fósseis da Formação Pirabas. *Divisão de Geologia e Mineralogia*, Departamento Nacional da Produção Mineral, **16**:1–35.
- Soares Jr. A.V., Hasui Y., Costa J.B.S., Machado F.B. 2011. Evolução do rifteamento e paleogeografia da margem Atlântica Equatorial do Brasil: Triássico ao Holoceno. *Geociências-UNESP*, **30**(4):669-692.
- Távora V.A. & Fernandes J. 1999. Estudio de los foraminiferos de la Formación Pirabas (Mioceno Inferior), Estado do Pará, Brasil, y su correlación com faunas del Caribe. *Revista Geológica de América Central*, **22**: 59–70.

Távora V.A., Silveira E.S.F., Milhomem Neto J.M. 2007. Mina B-17, Capanema,PA - expressivo registro de uma Paleolaguna do Cenozóico Brasileiro. *In: Winge M., Schobbenhaus C., Berbert-Born M., Queiroz E.T., Campos D.A., Souza C.R.G., Fernandes A.C.S. (ed.) Sítios geológicos e paleontológicos do Brasil*. Publicado na Internet em 07/01/2007 no endereço <http://www.unb.br/ig/sigep/sitio121/sitio121.pdf>.

Távora V.A., Imbeloni E.F.F., Cacela A. S. M., Baia N. M. 2004. Paleoinvertebrados. *In: Rossetti F. R. & Góes A.M. (ed). O Neógeno da Amazônia Oriental*. Belém, MPEG, p.111-131.

Tucker M.E. 1992. *Sedimentary petrology*. Blackwell Scientific Publications, 260p.

White C. A. 1887. Contribuições à paleontologia do Brasil. *Archivos do Museu Nacional*, **7**:1–273.